Geochemical Perspectives Letters

Contrasting oxygen isotopes in garnet from diamondiferous and barren eclogitic parageneses

N. Korolev[1,2*,†], M. Kopylova[1], E. Dubinina[3], R.A. Stern[4]

OPEN ACCESS

https://doi.org/10.7185/geochemlet.2328

Abstract

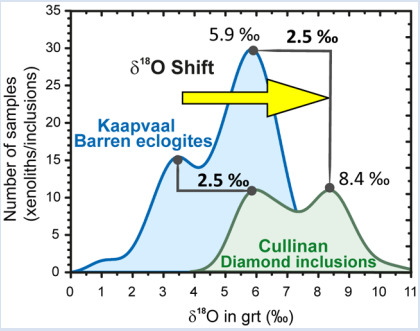

Eclogite is a minor mantle lithology, present in subducted slivers in cratonic roots. Mantle eclogites carry O and C isotopic signatures from surface organic and inorganic carbon and also are modified by reaction with fluids in the lithosphere. One third of the diamonds mined worldwide are sourced from mantle eclogites, and individual eclogite xenoliths contain up to 20 vol. % diamond. It is critically important to understand where the diamond carbon comes from, and how the diamonds form, for insights on the carbon cycle, diamond exploration, and processes in the lithospheric mantle. Few samples and methods are available to constrain diamond formation in eclogites; in this work we focus on oxygen isotopes in eclogitic garnets. New analyses of garnet/majorite found as inclusions in the Cullinan diamonds reveal a statistically significant systematic difference between $\delta^{18}O$ in garnet associated, and unassociated, with diamond. This contrast persists between garnet from diamondiferous and barren eclogite xenoliths and cannot be due to shielding of diamond inclusions from equilibrating with the common mantle values of $\delta^{18}O$. We propose that diamond-forming metasomatic reactions triggered by carbonatitic fluids may contribute up to 1.5 ‰ to the shift of $\delta^{18}O$ to higher values in eclogitic diamondiferous paragenesis, but cannot fully account for the observed difference of 2.5 ‰.

Received 16 May 2022 | Accepted 26 July 2023 | Published 6 September 2023

Introduction

Eclogite, a high grade garnet (Grt)-clinopyroxene (Cpx) rock metamorphosed from the mafic crust, is the most diamondiferous mantle lithology. Diamond concentrations in mantle eclogite can be orders of magnitude higher than the concentration of diamonds in kimberlite – the rock from which they are mined. Over the past 40 years, the oxygen isotope composition ($\delta^{18}O$) of eclogite has become one of the most powerful indicators of its crustal origin in the cratonic mantle (Schulze *et al.*, 2003), together with stable isotopes of C, N and S, and radiogenic isotopes (Pearson *et al.*, 2003; Jacob, 2004). Diamond growth, however, is envisioned as a process overprinting the recycled shallow eclogite protolith. Crustal protoliths for the eclogite do not necessarily imply crustal sources for its diamonds, which could inherit shallow C and O, or could be introduced to the eclogite from mantle fluids. A knowledge of diamond formation in eclogites is critically important to unravel the carbon cycle and deep mantle processes. Diamond formation is considered to be partly metasomatic, as suggested by diamond distribution in eclogites (Taylor and Anand, 2004), $\delta^{13}C$ core-to-rim patterns (Smart *et al.*, 2011) and correlations of O isotopes with trace element indicators of metasomatism (Gréau *et al.*, 2011; Huang *et al.*, 2012). Diamond precipitates from mantle C-bearing fluids percolating upward and experiencing Raleigh fractionation (Stachel and Luth, 2015; Riches *et al.*, 2016). Possible effects of metasomatic diamond formation on $\delta^{18}O$ of eclogitic minerals may be especially notable for diamondiferous parageneses. Our goal is to quantify these $\delta^{18}O$ to separate out the signatures of shallower crustal alteration from the changes introduced from deeper-seated diamondiferous fluids.

It has been noticed that garnet and clinopyroxene in diamondiferous eclogites are higher in $\delta^{18}O$ than their respective phases in barren eclogites (Pearson *et al.*, 2003). The difference was explained by the origin of garnet in diamondiferous assemblages from the shallow, more altered part of the oceanic crust where $\delta^{18}O$ is higher (McCulloch *et al.*, 1981; Alt *et al.*, 1986; Ickert *et al.*, 2013). This study aims to extend the comparison to eclogitic inclusions in diamonds and make it more statistically robust. In the last 20 years, advances in measurements of O isotopes and new kimberlite discoveries created an abundance of new data. A new summary on $\delta^{18}O$ in garnet from diamondiferous and barren parageneses is long overdue. Here we confirm the distinction between $\delta^{18}O$ of garnet equilibrated

1. University of British Columbia, 2207 Main Mall, Vancouver, BC V6T 1Z4, Canada
2. Institute of Precambrian Geology and Geochronology RAS, nab. Makarova 2, St. Petersburg 199034, Russia
3. Laboratory of Isotope Geochemistry and Geochronology, Institute of Geology of Ore Deposits, Petrography, Mineralogy and Geochemistry RAS, Staromonetny per. 35, Moscow 119017, Russia
4. Canadian Centre for Isotopic Microanalysis, Department of Earth and Atmospheric Sciences, University of Alberta, Edmonton, Alberta, T6G 2E3, Canada
† Current affiliation: University College Cork, School of Biological, Earth and Environmental Sciences, University College Cork, Distillery Fields, North Mall, Butler Building, Cork, T23 N73K, Ireland
* Corresponding author (email: nkorolev@ucc.ie)

and unequilibrated with diamond and assess how much of this distinction can be assigned to diamond-friendly metasomatism.

Samples, Methods and Results

We studied diamond inclusions (DIs) from Cullinan Mine (Premier kimberlite) individual raw diamonds. The inclusions are associated with mafic eclogitic and majorite-bearing sublithospheric parageneses. They are derived from a wide interval of temperatures (*T*) and pressures (*P*) of 5.5–7.5 GPa from the lithosphere and 10.5–13.5 GPa from the sublithospheric mantle (Korolev *et al.*, 2018a). Here we report major element, $\delta^{18}O$, and *P-T* data for 42 non-touching Grt-Cpx pairs and 8 majorites (Supplementary Information; Table S-5). Analysed $\delta^{18}O$ composition of garnet ranges from +5.4 to +10.2 ‰ and covers the oxygen isotope composition of majorites worldwide (+6.0 to +9.4 ‰; Burnham *et al.*, 2015; Ickert *et al.*, 2015).

This new dataset of O isotopes in eclogitic garnet DIs enables statistical comparison with global datasets. The most notable pattern is revealed by a comparison of $\delta^{18}O$ in garnet/majorite associated with diamond (DIs and diamondiferous eclogites) and garnet in barren eclogites. Statistical *t* tests determine that the average $\delta^{18}O$ and its distribution in garnet from diamondiferous eclogites are distinctly higher than the barren eclogites from the Kaapvaal craton with probability >99.99 % (Supplementary Information). The $\delta^{18}O$ compositions of the garnet/majorite inclusions from the Cullinan diamonds are higher than the $\delta^{18}O$ of garnet in Kaapvaal barren eclogites (Fig. 1a). While only 24 % of Cullinan DIs demonstrate $\delta^{18}O < +6$ ‰ and values <+5 ‰ are completely absent (Fig. 1a, Table S-5), 67.4 % of garnets from the barren eclogites have $\delta^{18}O < +6.0$ ‰. Diamondiferous eclogites globally show a narrow $\delta^{18}O$ distribution with a higher mode than the Kaapvaal barren eclogites (Fig. 1b).

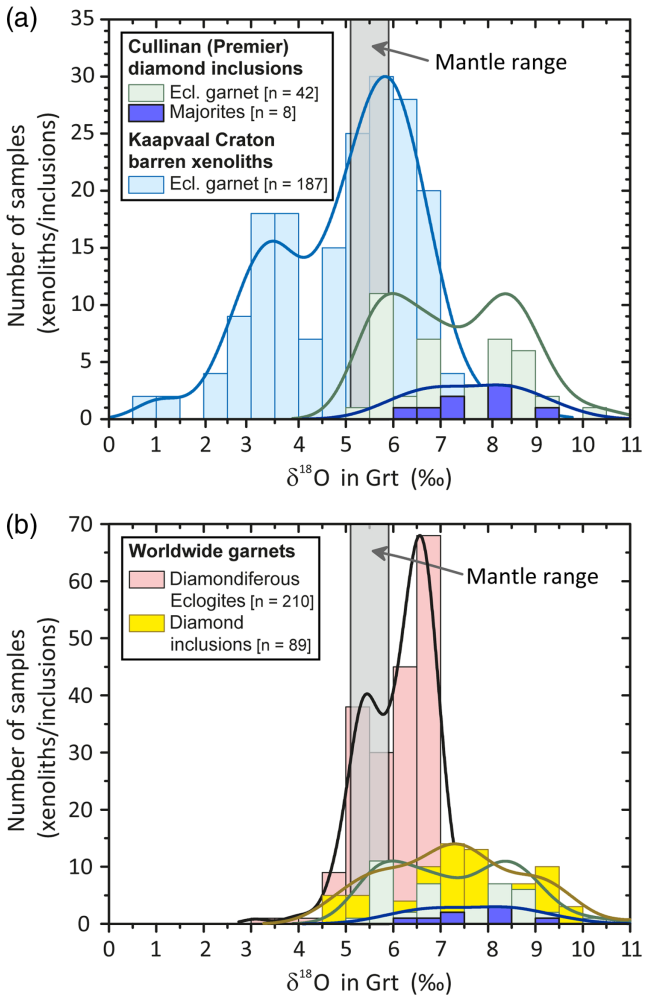

Figure 1 $\delta^{18}O$ histograms for eclogitic garnet in xenoliths and DIs. **(a)** Comparison of our data with Kaapvaal non-diamondiferous eclogites. **(b)** Comparison of global data for garnet/majorite DIs with garnets from diamondiferous eclogites worldwide (references are listed in the Supplementary Information). Lines are kernel-smoothed distribution curves.

Discussion

Several explanations may account for the contrasting $\delta^{18}O$ in barren and diamondiferous eclogitic parageneses. The latter may have formed deeper (>150 km), at higher pressures and temperatures. A suggested positive covariation of $\delta^{18}O_{grt}$ with equilibration temperature for Lace eclogites may hint at a wider *T*-$\delta^{18}O_{grt}$ correlation in the deep mantle as heavy oxygen may favour garnet with increasing *T* and *P* (Aulbach *et al.*, 2017). To test for this, we compiled data for eclogite xenoliths of the Kaapvaal craton (Fig. S-3a) and worldwide occurrences (Fig. S-4). The absence of $\delta^{18}O$ correlations of garnet DIs with the *P-T* of their formation observed in Cullinan (Fig. S-3) is repeated globally. A comparison of the $\delta^{18}O$ in Grt-Cpx pairs from eclogite xenoliths worldwide equilibrated at the widest range of temperatures (650–1500 °C) shows that there is no dependence between $\delta^{18}O_{grt}$ or $\delta^{18}O_{cpx}$ and temperature (Fig. S-4). The difference between $\delta^{18}O_{grt}$ and $\delta^{18}O_{cpx}$ is constant (±0.87 ‰, 2σ) and does not correlate with temperature (Fig. S-4a). The contrasting $\delta^{18}O$ compositions in barren and diamondiferous parageneses do not relate to pressure, which was predicted by Clayton *et al.* (1975). Only a small proportion of Cullinan Mg-rich DIs demonstrate a local $\delta^{18}O$-*T* correlation (Supplementary Information; Fig. S-2b). Thus, higher pressures and temperatures of diamondiferous eclogites and DIs cannot account for the heavier oxygen in their garnets.

An alternative explanation invokes diffusive buffering of oxygen by the surrounding mantle to explain the $\delta^{18}O$ contrast between garnet in barren (xenoliths) and diamondiferous eclogitic parageneses (DIs and xenoliths). DI garnet is shielded from re-equilibration with the ambient mantle oxygen ($\delta^{18}O = +5.5 \pm 0.4$ ‰; Mattey *et al.*, 1994), while the "exposed" garnet in xenoliths is not. Only silicate inclusions protected by diamonds retained the ^{18}O-enriched compositions (Schulze *et al.*, 2003; Burnham *et al.*, 2015; Ickert *et al.*, 2015) formed *via* low temperature seawater alteration of the shallowest levels of the former oceanic crust (McCulloch *et al.*, 1981; Alt *et al.*, 1986). These diamonds and their mineral inclusions originated from carbon and oxygen derived from the sedimentary organic matter or altered oceanic crust (Li *et al.*, 2019) subducted into the mantle, as evidenced by a correlation of heavy ^{18}O in silicate DIs and light, low $^{13}C/^{12}C$ carbon (Ickert *et al.*, 2015; Li *et al.*, 2019). The extent of this "diamond shielding" effect can be evaluated by comparing $\delta^{18}O$ histograms for garnet in DIs and diamondiferous eclogites. The $\delta^{18}O$ mode for the DI garnet is between +7 and +8 ‰, 1 ‰ higher than the mode for the exposed garnet in diamondiferous eclogites (Fig. 1b).

One cannot defer to the "diamond shielding" effect to explain the contrast between garnet compositions of diamondiferous and barren xenoliths. The latter show a mode at +5 to +6 ‰, at a lower $\delta^{18}O$ than diamondiferous xenoliths, and an extended "tail" of the distribution towards 0 ‰ (Fig. 1a). A clear difference in $\delta^{18}O$ was shown for both Cpx and Grt for barren and diamondiferous eclogites worldwide (Fig. 2). Traditionally,

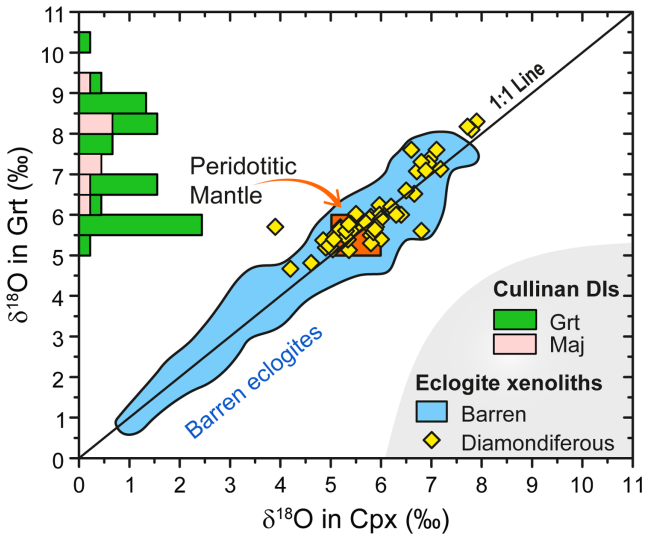

Figure 2 Comparison of $\delta^{18}O$ in eclogitic minerals for barren ($n = 183$) and diamondiferous ($n = 52$) parageneses worldwide (references are given in the Supplementary Information) with a superimposed histogram for $\delta^{18}O$ in the Cullinan DIs (this study).

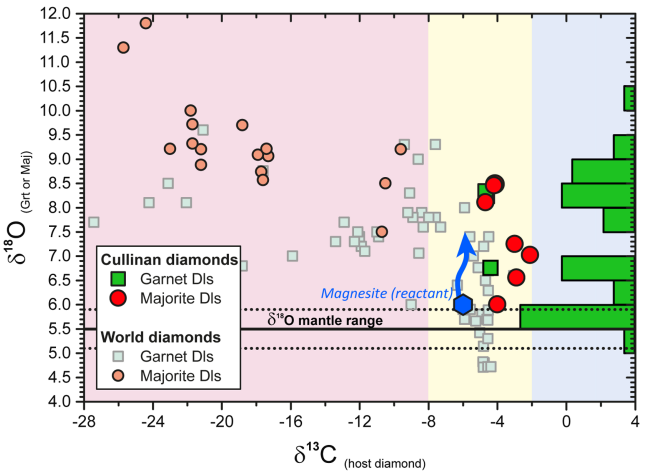

Figure 3 Comparison of $\delta^{18}O$ of eclogitic garnets/majorites and $\delta^{13}C$ of the host diamond worldwide (ESM1) with $\delta^{18}O$ of Cullinan diamond inclusions. Inclusions with $\delta^{13}C$ for studied Cullinan diamonds (Korolev *et al.*, 2018a) are plotted as symbols, $\delta^{18}O$ of eclogitic garnets with no information on the host diamond $\delta^{13}C$ are shown as the green histogram. The blue hexagon marks the initial magnesite reactant. A blue arrow connects $\delta^{18}O$ of the magnesite reactant with the Grt product for modelled combined metasomatic reactions (Reactions 1 and 8 in Table S-4); it is placed at an average mantle value of −6 ‰ for $\delta^{13}C$. The blue field corresponds to $\delta^{13}C$ in sedimentary carbonates, the yellow field represents mantle carbon, and the pink field is for organic carbon.

this difference would be explained as the contrast in $\delta^{18}O$ of the eclogite protoliths is related to their depth position within the slab and the gradual decrease of $\delta^{18}O$ with depth in the oceanic crust (McCulloch *et al.*, 1981; Alt *et al.*, 1986). In this model, garnet in barren eclogites might have inherited the $\delta^{18}O$ from deep gabbro layers of oceanic crust ($\delta^{18}O = 0$ to +5 ‰; Alt *et al.*, 1986). Diamondiferous eclogites with higher $\delta^{18}O$, by contrast, may have recorded a higher input from altered oceanic basalts ($\delta^{18}O = +7$ to +15 ‰; McCulloch *et al.*, 1981; Alt *et al.*, 1986; Eiler, 2001; Korolev *et al.*, 2018b).

The second model can explain light C and heavy O isotope compositions of many diamonds and their inclusions, where carbonate in altered mafic-ultramafic oceanic crust with $\delta^{18}O = +11$ to +33 ‰, $\delta^{13}C = -30$ to −5 ‰ (Li *et al.*, 2019) and organic C (Fig. 3) contributed to eclogite protoliths. Yet the Cullinan diamonds with eclogitic and sublithospheric majoritic inclusions have the characteristic mantle $\delta^{13}C$ of −2.4 to −4.8 ‰ (Fig. 3) indistinguishable from Cullinan peridotitic diamonds (Korolev *et al.*, 2018a). Thus, the model implying contribution of carbonate in altered mafic-ultramafic oceanic crust cannot be universally applied to all diamonds with inclusions enriched in heavy O, although the model adequately explains compositional patterns in many diamond occurrences.

Another factor that may contribute to contrasting $\delta^{18}O$ in barren and diamondiferous eclogites are diamond-forming metasomatic reactions. Metasomatism plays a central role in diamond formation (Stachel and Harris, 2008), and its effect on stable isotopes of diamondiferous parageneses ought to be quantitatively assessed. It was proposed that the metasomatism may have modified the eclogitic protolith by diffusional equilibration with a carbonatitic fluid (Lowry *et al.*, 1999) or with the mantle carbonatitic fluids containing heavy oxygen ($\delta^{18}O$ of +5 to +10.5 ‰) (Gréau *et al.*, 2011; Huang *et al.*, 2016). However, any fluid deviating from the mantle O isotopic composition is expected to be short lived, as it would be buffered back to the mantle $\delta^{18}O$ values by re-equilibration with ambient peridotite oxygen isotope reservoirs (Riches *et al.*, 2016).

We tested viable diamond-forming reactions that do not involve heavy oxygen-rich fluids for ^{18}O enrichment effects. Diamond can form by oxidation of methane-rich fluids, by reduction of carbonatitic fluids or by isochemical precipitation from cooling or ascending C-H-O fluids (Stachel and Luth, 2015). The isochemical precipitation would not shift $\delta^{18}O$, while oxidation of methane or other reduced fluids equilibrated with H_2O would lead to metasomatic silicates with lighter oxygen compositions (Ickert *et al.*, 2013). An origin of diamond from an oxidised medium was suggested on the basis of the core-to-rim increases in $\delta^{13}C$ composition of individual diamonds (Smart *et al.*, 2011) and daughter minerals in fluid inclusions in diamonds (Kopylova *et al.*, 2010). We modelled $\delta^{18}O$ effects for metasomatism by oxidising fluids in multiple feasible reactions with the realistic eclogitic mineralogy. The reactions start with the carbonatitic fluid equilibrated with the initial eclogitic garnet ($\delta^{18}O = +6.0$ ‰) and leads to a $\delta^{18}O$ value of resulting garnet elevated by as much as 1.5 ‰ (Fig. 4; Supplementary Information). Diamond-forming metasomatising reactions with the strongest $\delta^{18}O$ shift upward involve 1) production of O_2 or CO_2, 2) heavy oxygen supplied by the metasomatic fluid, 3) a sufficiently high fluid/rock ratio (1–3 moles of fluid to 1 mole of garnet), and 4) oxides (rutile or ilmenite) as products rather than reactants. In Reactions 1 and 2 (Table S-4), diamond forms by disproportionation also creating free O_2, which is immediately used up to make Fe^{3+}-bearing Grt and Cpx (Reaction 8; Table S-4). Reactions 3–7 (Table S-4) facilitate diamond production indirectly, by adding carbon dioxide to C-O-H mantle fluids that may be parental to diamonds (Stachel *et al.*, 2022). The CO_2 concentrations in the mantle, however, are expected to be low, buffered by silicate carbonation (Kopylova *et al.*, 2021). In CO_2 producing reactions the $\delta^{18}O$ of product garnet is elevated by 0.5 to 0.6 ‰ (Table S-4), and the strongest $\delta^{18}O$ upward shift of 1.5 ‰ is observed as a net effect of Reaction 1:

$$\text{Almandine} + 3 \cdot \text{Magnesite} = \text{Pyrope} + \text{Magnetite} + 3 \cdot \text{C} + 2.5 \cdot \text{O}_2$$

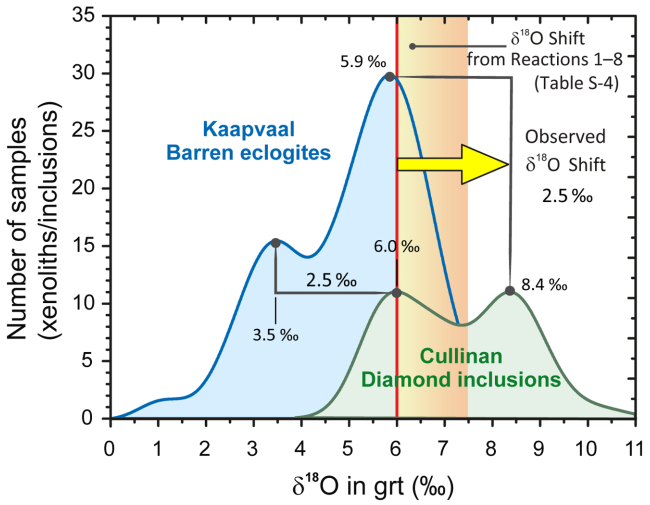

Figure 4 The observed $\delta^{18}O$ contrast between barren and diamondiferous eclogites with superimposed modelled changes of $\delta^{18}O$ composition of eclogitic garnets produced in metasomatic reactions (orange field; Table S-4). The initial $\delta^{18}O$ in eclogitic garnet (vertical line at +6 ‰) is chosen arbitrarily (see explanations in the text). A detailed description of the geochemical modelling is provided in the Supplementary Information.

followed by Reaction 8:

$$2 \cdot \text{Grt} + 13.5 \cdot \text{Cpx} + 0.5 \cdot O_2 = 3 \cdot \text{Fe}^{3+}\text{-bearing Grt} + 11 \cdot \text{Fe}^{3+}\text{-bearing Cpx} + 2 \cdot \text{Quartz(Coesite)}.$$

All phases in the proposed reactions are found in cratonic eclogites (*e.g.*, Jacob, 2004), and the latter reaction is based on the observed concentrations of Fe^{3+} in eclogitic minerals (Aulbach *et al.*, 2022). A replacement of eclogitic garnet with a more magnesian garnet has been described in multiple occurrences as part of diamond-friendly metasomatism (*e.g.*, De Stefano *et al.*, 2009; Korolev *et al.*, 2021). An increase of MgO was found to be the most significant chemical change accompanying $\delta^{18}O$ enrichment in garnet from Orapa eclogite xenoliths (Deines *et al.*, 1991). It is well known that metasomatism oxidises the adjacent metasomatised mantle (Creighton *et al.*, 2009). The reactions are equally applicable to majorites in the sublithospheric mantle (Supplementary Information).

We conclude that some metasomatic reactions of diamond formation in eclogites may contribute to the observed $\delta^{18}O$ contrast between barren and diamondiferous eclogitic assemblages worldwide, yet the strongest upward $\delta^{18}O$ shift of all feasible metasomatic reactions (up to 1.5 ‰) achieved in decarbonation followed by metasomatic oxidation is not sufficient to explain the 2.5 ‰ difference in $\delta^{18}O$ (Fig. 4). Inheritance of the O isotopic composition from the crustal eclogitic protoliths is the only model that currently offers a satisfactory explanation for the contrast. This implies preferential diamond formation in eclogites with shallow basaltic protoliths with or without contribution of carbonate in altered mafic-ultramafic oceanic crust that experienced stronger low temperature alteration on the seafloor.

Acknowledgements

We are grateful to J. Davidson (Petra Diamonds), J. Gurney and A. Moore for donation of diamonds for the research. It was funded by NSERC Discovery grant 2019-03988 to MK and by RNF grant № 22-17-00052 to ED. We express our gratitude to Horst R. Marschall, Steven Shirey and an anonymous reviewer for their constructive comments on the manuscript.

Editor: Horst R. Marschall

Additional Information

Supplementary Information accompanies this letter at https://www.geochemicalperspectivesletters.org/article2328.

Cite this letter as: Korolev, N., Kopylova, M., Dubinina, E., Stern, R.A. (2023) Contrasting oxygen isotopes in garnet from diamondiferous and barren eclogitic parageneses. *Geochem. Persp. Let.* 27, 15–19. https://doi.org/10.7185/geochemlet.2328

References

Alt, J.C., Muehlenbachs, K., Honnorez, J. (1986) An oxygen isotopic profile through the upper kilometer of the oceanic crust, DSDP Hole 504B. *Earth and Planetary Science Letters* 80, 217–229. https://doi.org/10.1016/0012-821X(86)90106-8

Aulbach, S., Woodland, A.B., Vasilyev, P., Galvez, M.E., Viljoen, K.S. (2017) Effects of low-pressure igneous processes and subduction on $Fe^{3+}/\Sigma Fe$ and redox state of mantle eclogites from Lace (Kaapvaal craton). *Earth and Planetary Science Letters* 474, 283–295. https://doi.org/10.1016/j.epsl.2017.06.030

Aulbach, S., Woodland, A.B., Stagno, V., Korsakov, A.V., Mikhailenko, D., Golovin, A. (2022) Fe^{3+} Distribution and $Fe^{3+}/\Sigma Fe$-Oxygen Fugacity Variations in Kimberlite-Borne Eclogite Xenoliths, with Comments on Clinopyroxene-Garnet Oxy-Thermobarometry. *Journal of Petrology* 63, egac076. https://doi.org/10.1093/petrology/egac076

Burnham, A.D., Thomson, A.R., Bulanova, G.P., Kohn, S.C., Smith, C.B., Walter, M.J. (2015) Stable isotope evidence for crustal recycling as recorded by superdeep diamonds. *Earth and Planetary Science Letters* 432, 374–380. https://doi.org/10.1016/j.epsl.2015.10.023

Clayton, R.N., Goldsmith, J.R., Karel, K.J., Mayeda, T.K., Newton, R.C. (1975) Limits on the effect of pressure on isotopic fractionation. *Geochimica et Cosmochimica Acta* 39, 1197–1201. https://doi.org/10.1016/0016-7037(75)90062-9

Creighton, S., Stachel, T., Matveev, S., Höfer, H., McCammon, C., Luth, R.W. (2009) Oxidation of the Kaapvaal lithospheric mantle driven by metasomatism. *Contributions to Mineralogy and Petrology* 157, 491–504. https://doi.org/10.1007/s00410-008-0348-3

Deines, P., Harris, J.W., Robinson, D.N., Gurney, J.J., Shee, S.R. (1991) Carbon and oxygen isotope variations in diamond and graphite eclogites from Orapa, Botswana, and the nitrogen content of their diamonds. *Geochimica et Cosmochimica Acta* 55, 515–524. https://doi.org/10.1016/0016-7037(91)90009-T

De Stefano, A., Kopylova, M.G., Cartigny, P., Afanasiev, V. (2009) Diamonds and eclogites of the Jericho kimberlite (Northern Canada). *Contributions to Mineralogy and Petrology* 158, 295–315. https://doi.org/10.1007/s00410-009-0384-7

Eiler, J.M. (2001) Oxygen Isotope Variations of Basaltic Lavas and Upper Mantle Rocks. *Reviews in Mineralogy and Geochemistry* 43, 319–364. https://doi.org/10.2138/gsrmg.43.1.319

Gréau, Y., Huang, J.-X., Griffin, W.L., Renac, C., Alard, O., O'Reilly, S.Y. (2011) Type I eclogites from Roberts Victor kimberlites: Products of extensive mantle metasomatism. *Geochimica et Cosmochimica Acta* 75, 6927–6954. https://doi.org/10.1016/j.gca.2011.08.035

Huang, J.-X., Gréau, Y., Griffin, W.L., O'Reilly, S.Y., Pearson, N.J. (2012) Multi-stage origin of Roberts Victor eclogites: Progressive metasomatism and

its isotopic effects. *Lithos* 142–143, 161–181. https://doi.org/10.1016/j.lithos.2012.03.002

Huang, J.-X., Xiang, Y., An, Y., Griffin, W.L., Gréau, Y., Xie, L., Pearson, N.J., Yu, H., O'Reilly, S.Y. (2016) Magnesium and oxygen isotopes in Roberts Victor eclogites. *Chemical Geology* 438, 73–83. https://doi.org/10.1016/j.chemgeo.2016.05.030

Ickert, R.B., Stachel, T., Stern, R.A., Harris, J.W. (2013) Diamond from recycled crustal carbon documented by coupled $\delta^{18}O$–$\delta^{13}C$ measurements of diamonds and their inclusions. *Earth and Planetary Science Letters* 364, 85–97. https://doi.org/10.1016/j.epsl.2013.01.008

Ickert, R.B., Stachel, T., Stern, R.A., Harris, J.W. (2015) Extreme ^{18}O-enrichment in majorite constrains a crustal origin of transition zone diamonds. *Geochemical Perspectives Letters* 1, 65–74. https://doi.org/10.7185/geochemlet.1507

Jacob, D.E. (2004) Nature and origin of eclogite xenoliths from kimberlites. *Lithos* 77, 295–316. https://doi.org/10.1016/j.lithos.2004.03.038

Kopylova, M., Navon, O., Dubrovinsky, L., Khachatryan, G. (2010) Carbonatitic mineralogy of natural diamond-forming fluids. *Earth and Planetary Science Letters* 291, 126–137. https://doi.org/10.1016/j.epsl.2009.12.056

Kopylova, M.G., Ma, F., Tso, E. (2021) Constraining carbonation freezing and petrography of the carbonated cratonic mantle with natural samples. *Lithos* 388–389, 106045. https://doi.org/10.1016/j.lithos.2021.106045

Korolev, N., Kopylova, M., Gurney, J.J., Moore, A.E., Davidson, J. (2018a) The origin of Type II diamonds as inferred from Cullinan mineral inclusions. *Mineralogy and Petrology* 112, 275–289. https://doi.org/10.1007/s00710-018-0601-z

Korolev, N.M., Melnik, A.E., Li, X.-H., Skublov, S.G. (2018b) The oxygen isotope composition of mantle eclogites as a proxy of their origin and evolution: A review. *Earth-Science Reviews* 185, 288–300. https://doi.org/10.1016/j.earscirev.2018.06.007

Korolev, N., Nikitina, L.P., Goncharov, A., Dubinina, E.O., Melnik, A., Müller, D., Chen, Y.-X., Zinchenko, V.N. (2021) Three Types of Mantle Eclogite from Two Layers of Oceanic Crust: A Key Case of Metasomatically-Aided Transformation of Low-to-High-Magnesian Eclogite. *Journal of Petrology* 62, egab070. https://doi.org/10.1093/petrology/egab070

Li, K., Li, L., Pearson, D.G., Stachel, T. (2019) Diamond isotope compositions indicate altered igneous oceanic crust dominates deep carbon recycling. *Earth and Planetary Science Letters* 516, 190–201. https://doi.org/10.1016/j.epsl.2019.03.041

Lowry, D., Mattey, D.P., Harris, J.W. (1999) Oxygen isotope composition of syngenetic inclusions in diamond from the Finsch Mine, RSA. *Geochimica et Cosmochimica Acta* 63, 1825–1836. http://dx.doi.org/10.1016/S0016-7037(99)00120-9

Mattey, D., Lowry, D., Macpherson, C. (1994) Oxygen isotope composition of mantle peridotite. *Earth and Planetary Science Letters* 128, 231–241. https://doi.org/10.1016/0012-821X(94)90147-3

McCulloch, M.T., Gregory, R.T., Wasserburg, G.J., Taylor Jr., H.P. (1981) Sm-Nd, Rb-Sr, and $^{18}O/^{16}O$ isotopic systematics in an oceanic crustal section: Evidence from the Samail ophiolite. *Journal of Geophysical Research: Solid Earth* 86, 2721–2735. https://doi.org/10.1029/JB086iB04p02721

Pearson, D.G., Canil, D., Shirey, S.B. (2003) 2.05 - Mantle Samples Included in Volcanic Rocks: Xenoliths and Diamonds. In: Holland, H.D., Turekian, K.K. (Eds.) *Treatise on Geochemistry*. First Edition, Elsevier, Amsterdam, 171–275. https://doi.org/10.1016/B0-08-043751-6/02005-3

Riches, A.J.V., Ickert, R.B., Pearson, D.G., Stern, R.A., Jackson, S.E., Ishikawa, A., Kjarsgaard, B.A., Gurney, J.J. (2016) *In situ* oxygen-isotope, major-, and trace-element constraints on the metasomatic modification and crustal origin of a diamondiferous eclogite from Roberts Victor, Kaapvaal Craton. *Geochimica et Cosmochimica Acta* 174, 345–359. https://doi.org/10.1016/j.gca.2015.11.028

Schulze, D.J., Harte, B., Valley, J.W., Brenan, J.M., Channer, D.M.D.R. (2003) Extreme crustal oxygen isotope signatures preserved in coesite in diamond. *Nature* 423, 68–70. https://doi.org/10.1038/nature01615

Smart, K.A., Chacko, T., Stachel, T., Muehlenbachs, K., Stern, R.A., Heaman, L.M. (2011) Diamond growth from oxidized carbon sources beneath the Northern Slave Craton, Canada: A $\delta^{13}C$–N study of eclogite-hosted diamonds from the Jericho kimberlite. *Geochimica et Cosmochimica Acta* 75, 6027–6047. https://doi.org/10.1016/j.gca.2011.07.028

Stachel, T., Harris, J.W. (2008) The origin of cratonic diamonds — Constraints from mineral inclusions. *Ore Geology Reviews* 34, 5–32. https://doi.org/10.1016/j.oregeorev.2007.05.002

Stachel, T., Luth, R.W. (2015) Diamond formation — Where, when and how? *Lithos* 220–223, 200–220. https://doi.org/10.1016/j.lithos.2015.01.028

Stachel, T., Cartigny, P., Chacko, T., Pearson, D.G. (2022) Carbon and Nitrogen in Mantle-Derived Diamonds. *Reviews in Mineralogy and Geochemistry* 88, 809–875. https://doi.org/10.2138/rmg.2022.88.15

Taylor, L.A., Anand, M. (2004) Diamonds: time capsules from the Siberian Mantle. *Geochemistry* 64, 1–74. https://doi.org/10.1016/j.chemer.2003.11.006

Geochemical Perspectives Letters

Contrasting oxygen isotopes in garnet from diamondiferous and barren eclogitic parageneses

N. Korolev, M. Kopylova, E. Dubinina, R.A. Stern

Supplementary Information

The Supplementary Information includes:

- Analytical Methods
- Samples and Results
- Supplementary Tables S-1 to S-5
- Supplementary Figures S-1 to S-4
- References for Figures 1, S-3 and S-4, and Table S-2
- References for Figure 2
- Supplementary Information References

Analytical Methods

Diamond Polishing

Diamond inclusions (DIs) were analysed on polished diamond surfaces *in situ*. Host diamonds have been polished at the Department of Earth, Ocean and Atmospheric Sciences (EOAS) of the University of British Columbia (Vancouver, Canada) using a steel scaif impregnated with diamond powder. No natural or synthetic abrasive material was used for polishing.

Major-element Compositions of the Cullinan DIs: Microprobe Analysis

Major element composition of the exposed inclusions was analysed on a CAMECA SX-50 electron microprobe at EOAS, UBC. The studied samples were coated with carbon, analysed with a beam current of 20 nA, an acceleration voltage of 15 kV, and a peak count time of 20 s (except for K in pyroxene [40 s] and Na in garnet [60 s]); two backgrounds on either side of the peak were counted for 10 s (except for K in pyroxene [20 s] and Na in garnet [30 s]). The diameter of the electron beam was ~5 μm. The following standards, X-ray lines and crystals were used for garnet: albite, Na Kα, TAP; pyrope, Mg Kα, TAP; pyrope, Al Kα, TAP; pyrope, Si Kα, TAP; pyrope, Ca Kα, PET. For the elements considered in pyroxene analyses, the following standards, X-ray lines and crystals were used: albite, Na Kα, TAP; kyanite, Al Kα, TAP; diopside, Mg Kα, TAP; diopside, Si Kα, TAP; orthoclase, K Kα, PET; diopside, Ca Kα, PET; rutile, Ti Kα, PET; synthetic magnesiochromite, Cr Kα, LIF; synthetic rhodonite, Mn Kα, LIF; synthetic fayalite, Fe Kα, LIF. The 'PAP' $\phi(\rho Z)$ method (Pouchou and Pichoir, 1991) has been applied for the data reduction. Detection limits

are given in Table S-1. Fe^{3+} content was calculated stoichiometrically on the basis of the ideal oxygen unit total for each respective mineral. Chemical compositions of the studied inclusions and related information are given in Table S-5.

Table S-1 Calculated minimum detection limits in wt. % (MDL) for the Cullinan diamond inclusions.

Elements	Grt	Cpx
SiO_2	0.06	0.06
TiO_2	0.05	0.05
Al_2O_3	0.04	0.04
Cr_2O_3	0.07	0.07
FeO	0.08	0.07
MnO	0.07	0.07
MgO	0.03	0.03
CaO	0.04	0.04
Na_2O	0.02	0.02
K_2O	-	0.02

Raman Spectroscopy of the Cullinan DIs

Raman spectra of the mineral inclusions from diamonds were obtained with a Horiba XploRA PLUS confocal Raman spectrometer equipped with a CCD-detector at EOAS, UBC (Vancouver, Canada). Spectra have been collected at room temperature with the 532.18 nm line of a 14 mW Nd-YAG laser through an OLYMPUSTM 100X objective in the range between 100 and 1500–1800 cm^{-1} at 1.3 cm^{-1} spectral resolution, and ~1 µm spatial resolution. The aperture of the confocal hole was set to 200 µm, the spectra slit width was 300 µm.

Oxygen Isotope Compositions of the Cullinan DIs: Secondary Ion Mass Spectrometry (SIMS)

Oxygen isotope composition was measured in 50 eclogitic garnet and majorite inclusions (Table S-5).

Preparation of mounts and SIMS study of the samples were conducted at the Canadian Centre for Isotopic Microanalysis (CCIM), University of Alberta. Polished diamonds with the exposed majorite and garnet inclusions were arrayed on a tape and cast in 25 mm diameter epoxy mounts (M1612, M1613) along with CCIM garnet reference materials (RMs) S0068 (Gore Mountain Ca-Mg-Fe garnet), and S0088B (grossularite). The prepared mounts were cleaned with a lab soap solution and de-ionised H_2O. The studied samples were coated with 25 nm of high-purity Au prior to scanning electron microscopy (SEM). The SEM observations were made with a Zeiss EVO MA15 electron microscope using beam conditions of 20 kV and 3–4 nA. Coating of 100 nm of Au was subsequently deposited on the mount before SIMS analysis.

The oxygen isotope analysis (^{18}O, ^{16}O) of garnets was conducted using a Cameca IMS 1280 multicollector ion microprobe. Garnet analytical methods and RMs are reported in detail by Ickert and Stern (2013). A $^{133}Cs^+$ primary beam was operated with impact energy of 20 keV, and beam current of ~2.0 nA. The probe with the diameter of ~8 µm was rastered (20 × 20 µm) for 30 s prior to acquisition, and then 3 × 3 µm during acquisition, forming elliptical analysed areas ~12 µm across and ~1 µm deep. The normal incidence electron gun was utilised for charge compensation. Negative secondary ions were extracted through 10 kV potential into the secondary (Transfer) column. Transfer conditions

included a 122 µm entrance slit, a 5 × 5 mm pre-ESA (field) aperture, and 133× sample magnification at the field aperture, transmitting all regions of the sputtered area. The mass/charge separated oxygen ions were detected simultaneously in Faraday cups L'2 ($^{16}O^-$) and H'2 ($^{18}O^-$) at mass resolutions (m/Δm at 10 %) of 1950 and 2250, respectively. Secondary ion count rates for $^{16}O^-$ and $^{18}O^-$ were typically 2 × 10^9 and 4 × 10^6 counts/s utilising 10^{10} Ω and 10^{11} Ω amplifier circuits, respectively. Faraday cup baselines were measured at the start of the analytical session. A single analysis took 240 s, including pre-analysis primary beam implantation, automated secondary ion tuning, and 75 s of continuous peak counting.

Instrumental mass fractionation (IMF) was monitored by repeated analysis of S0068 (UAG) and S0088B with $\delta^{18}O_{VSMOW}$ = +5.72 ‰ and +4.13 ‰, respectively. One analysis of S0068 was taken after every four measurements, and one analysis of S0088B was taken after every eight unknowns. The data set of $^{18}O^-/^{16}O^-$ for S0068 garnet was processed collectively for two analytical sessions, yielding standard deviations of 0.10–0.13 ‰ after correction for systematic within-session drift. Data for S0088B and unknowns were first IMF corrected to S0068 garnet, and then further corrected according to their measured Ca#'s (Ca / [Ca + Mg + Fe]) using the methods suggested by Ickert and Stern (2013). The quadratic matrix calibration curve parameters (Ickert and Stern, 2013) were scaled to fit S0088B to its reference value. The 95 % confidence uncertainty estimates for $\delta^{18}O_{VSMOW}$ for garnet unknowns average ±0.30 ‰, and include errors relating to within-spot counting statistics, between-spot (geometric) effects, correction for instrumental mass fractionation, and matrix effects relating to Ca#s determined by electron microprobe wavelength dispersive spectrometry.

All $^{18}O/^{16}O$ ratios are reported in per mil (‰) and expressed in delta notation ($\delta^{18}O$) relative to Vienna Standard Mean Ocean Water (VSMOW) (Baertschi, 1976) in Equation S-1:

$$\delta^{18}O\ (‰) = [(^{18}O/^{16}O)_{sample} / (^{18}O/^{16}O)_{VSMOW}] - 1 \qquad \text{(Eq. S-1)}$$

Because the study jointly uses $\delta^{18}O$ values from SIMS and older laser fluorination analyses, it is important to establish their consistency. New data for Roberts Victor eclogitic garnet (Hardman *et al.*, 2021) (Fig. S-1) demonstrate that O isotope measurements by SIMS at the Canadian Centre for Isotopic Microanalysis (CCIM) and laser fluorination (LF) techniques are reproducible with the maximal discrepancy of ±0.35 ‰.

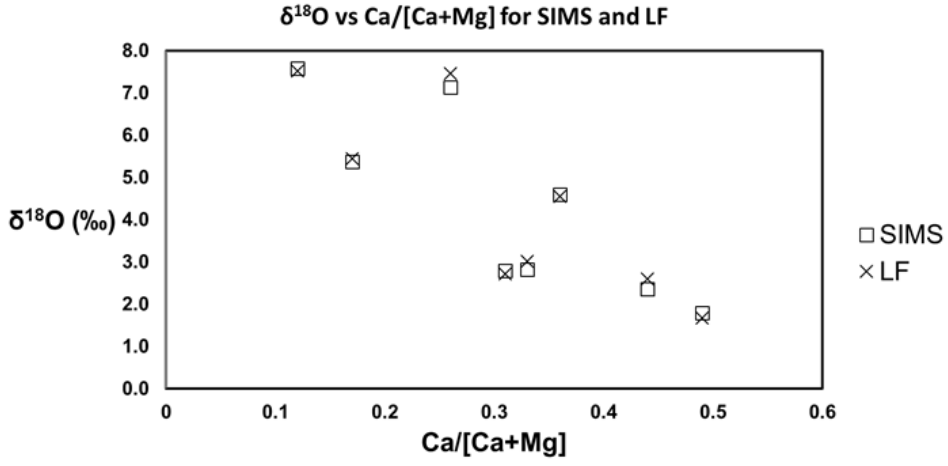

Figure S-1 Reproducibility test for O isotope measurements by SIMS at the Canadian Centre for Isotopic Microanalysis (CCIM), University of Alberta and laser fluorination (LF) techniques for garnet in Roberts Victor eclogites (Hardman *et al.*, 2021).

Samples and Results

Mineral Inclusions from the Cullinan Diamonds

We studied DI in mafic mineral parageneses (eclogitic and majorite-bearing parageneses of the transition zone) from diamonds of the Cullinan mine (Premier kimberlite), South Africa. This location was chosen because its slab-related diamonds formed from the single carbon source with narrow C isotope composition ($\delta^{13}C$ of 45 samples = −1.3 to −7.8 ‰), but derive from a wide interval of pressures (*P*) and temperatures (*T*) (Korolev *et al.*, 2018a, 2018b). Mineral inclusions come from depths of ~170–220 km (Grt and Cpx), 280–420 km (majorites) (Korolev *et al.*, 2018a, 2018b) and >550 km (CaSi-perovskite) (Nestola *et al.*, 2018), covering the broad *T* range in the lithospheric mantle from 1280 °C up to super-adiabatic 1570 °C (5.6–7.2 GPa) (Korolev *et al.*, 2018a, 2018b). To extend these intervals, we screened the Cullinan diamonds for more coexisting Grt-Cpx pairs and majorites that make the diamonds amenable to thermobarometry. As a result, we analysed 42 Grt-Cpx pairs and 8 majorites and calculated their *P*-*T*s of formation. This number of analyses and their respective *P*-*T*s are the highest reported for eclogitic diamonds from a single kimberlite. The inclusions were analysed for major elements; 50 garnets and majorites were further analysed for oxygen isotopes.

Analysed $\delta^{18}O$ compositions of garnet cover a range of +5.4 to +10.2 ‰ that includes the oxygen isotope composition of majorites (+6.0 to +9.4 ‰, Table S-5), indicating that the oxygen isotope composition does not change during slab transfer from the lithospheric to the sublithospheric mantle. Garnets and majorites show no correlation of the O isotopes with *T* or *P*, except a small subset of Mg-rich garnets coexisting with Cpx low in jadeitic component (Figs. S-2a and S-3).

Covariations of $\delta^{18}O$ with Thermodynamic Parameters of DIs

$\delta^{18}O$ shows a bimodal distribution with the first peak of around +6.0 ‰ and the other at +8.4 ‰ (green line on Fig. S-2). Garnets with $\delta^{18}O > 7.0$ ‰ show no correlation of the O isotopes with *T*. Garnets with the lighter O ($\delta^{18}O < 7.0$ ‰) can be divided into two groups, associated with the highly jadeitic (Jd) cpx (Jd > 40 %) or not (Fig. S-2b). MgO content of garnets in association with the high-Jd cpx is lower (7.2–12 wt. %, the median is 10.8 wt. %) than MgO content of the other garnets (9.2–17.4 wt. %, the median is 14.1 wt. %; Table S-5). The Mg-poor garnets associated with high-Jd cpx do not demonstrate a $\delta^{18}O$–*T* correlation, while Mg-rich garnets coexisting with low-Jd Cpx show a pronounced $\delta^{18}O$–*T* correlation (PCC = 0.72) (Fig. S-2a). The Mg-poor garnets associated with high-jadeitic Cpx are sourced from a variety of temperatures (Fig. S-2a) and pressures. There is no correlation between *P* and the oxygen isotope composition of garnets and majorites. Although we did not find any global correlation between *T* or *P* and $\delta^{18}O$ in garnet, the $\delta^{18}O$–*T* correlation is observed for Mg-rich garnets coexisting with low-Jd Cpx (Fig. S-2a). This correlation, along with analogous data on the Orapa and Lace mantle eclogite xenoliths (Deines *et al.*, 1991; Aulbach *et al.*, 2017) point to occasional presence of correlations restricted to a subset of samples (14 Cullinan inclusions (Fig. S-2a), 13 Lace eclogites (Aulbach *et al.*, 2017), and 12 Orapa eclogites (Deines *et al.*, 1991)). Notably, the $\delta^{18}O$–*T* correlation relates to the chemical composition of the Cullinan DIs, but also occurs in samples with $\delta^{18}O < 7$ ‰ (Fig. S-2a).

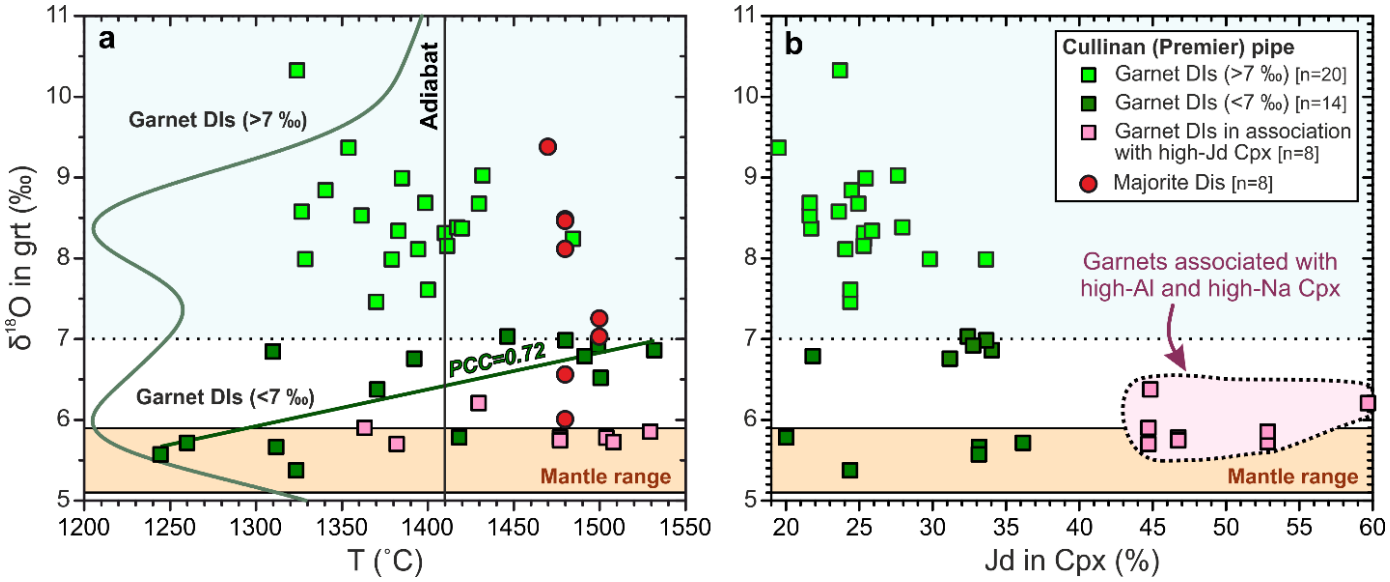

Figure S-2 Covariations of the oxygen isotope compositions for garnets in studied Cullinan diamonds with **(a)** calculated Cpx-Grt DI temperatures (Nakamura, 2009; adiabat after Katsura *et al*., 2010) and **(b)** jadeitic content of the coexisting DI Cpx. Here and on figures below the beige colour strip is the $\delta^{18}O$ mantle value canonical mantle range (5.5 ± 0.4 ‰) (Mattey *et al.*, 1994). PCC stands for the Pearson Correlation Coefficient.

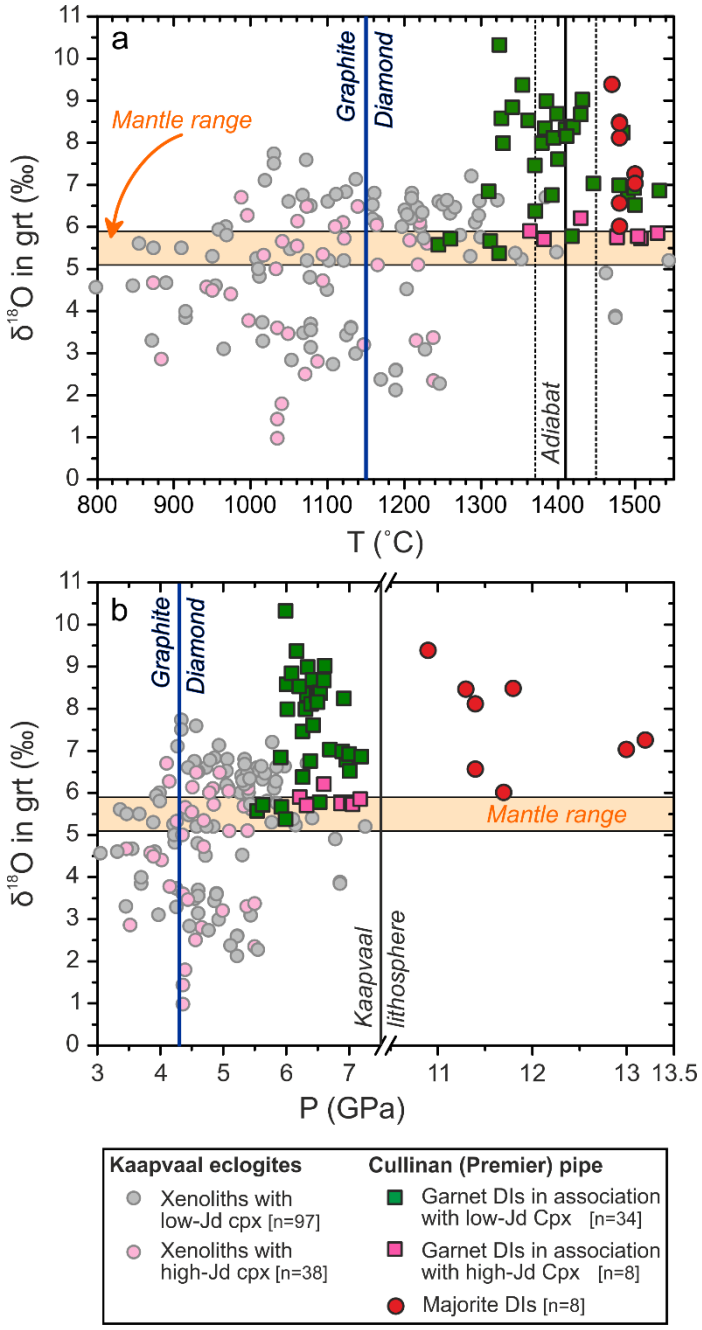

Figure S-3 Covariations of the oxygen isotope compositions with temperature and pressure for eclogitic Kaapvaal garnets in comparison with the studied Cullinan diamonds. **(a)** The garnet $\delta^{18}O$ *vs*. calculated Cpx-Grt temperatures (Nakamura, 2009). The temperatures for Kaapvaal eclogite xenoliths (see the database in Table S-5) were recalculated (Nakamura, 2009) for consistency; adiabat is after Katsura *et al.* (2010). **(b)** The $\delta^{18}O$ *vs*. estimated *P*. The pressure for Kaapvaal eclogites and Cullinan DIs is calculated by projection of the Cpx-Grt temperatures (Nakamura, 2009) onto the peridotitic geotherm as detailed in Korolev *et al.* (2018b). Full list of references on major element analyses of Cpx and Grt, and $\delta^{18}O$ in garnet is given below. The graphite-diamond phase boundary (Day, 2012) is shown by the blue line. It is positioned for the Kaapvaal craton at the intersection with the 40 mW/m^2 model conductive geotherm (Hasterok and Chapman, 2011).

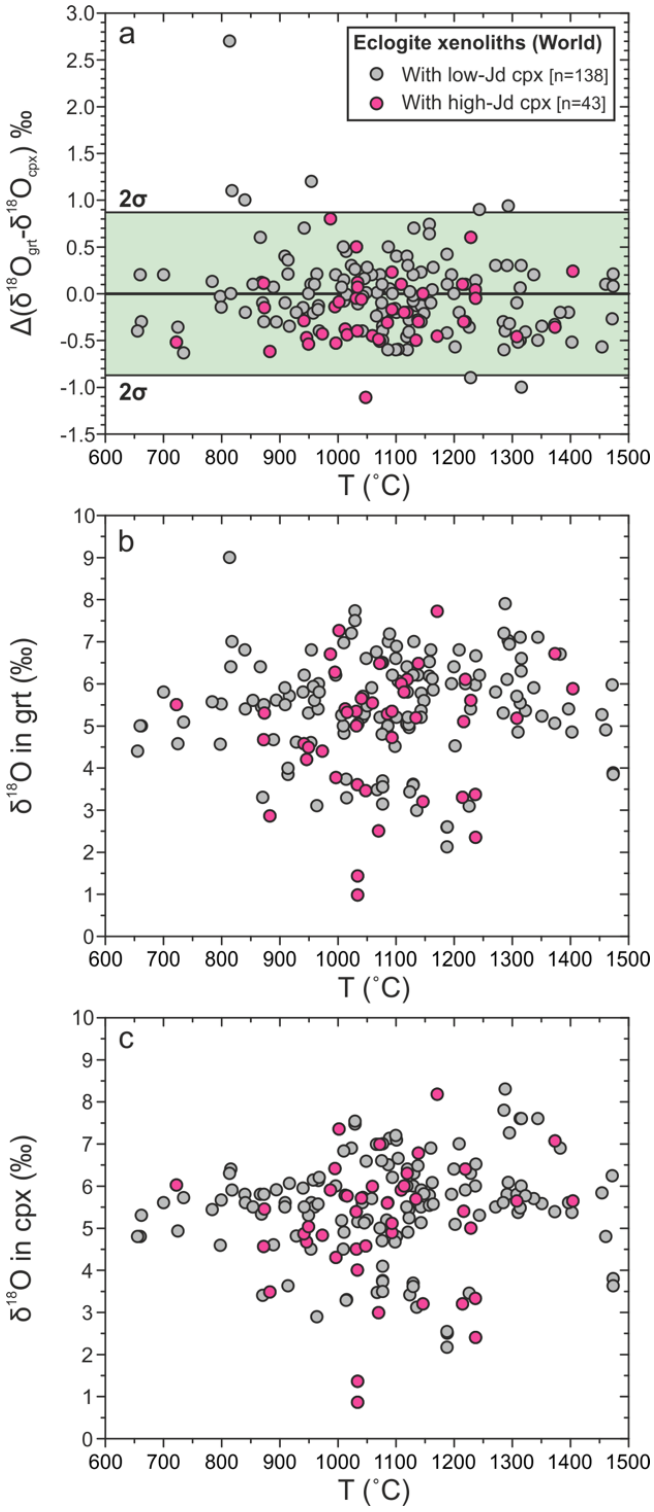

Figure S-4 Covariation between temperature and $\delta^{18}O$ composition for garnet and clinopyroxene from eclogite xenoliths worldwide. **(a)** The difference in oxygen isotope composition between garnet and clinopyroxene *vs*. temperature for 181 pairs; the difference between $\delta^{18}O_{grt}$ and $\delta^{18}O_{cpx}$ is ±0.87 ‰ (2σ; green area). **(b)** A plot of $\delta^{18}O_{grt}$ *vs*. T. **(c)** A plot of $\delta^{18}O_{grt}$ *vs*. pressure. The full list of references is given below.

Oxygen isotope composition of Cullinan majorites vs. DI majorites worldwide

All majorites that occur as diamond inclusions show relatively high $\delta^{18}O$ values well above the conventional mantle range (Fig. 3). The analysed majorites from Figure 3 include the Cullinan samples presented in this study (7 samples), DI from Jagersfontein (11 samples, Ickert *et al*., 2015), Juina-5 (3 samples, Burnham *et al*., 2015), and Collier-4 (3 samples, Burnham *et al*., 2015) diamonds. Majorites from Cullinan diamonds are notable because of their contrasting O isotope signatures. Majorites with heavy oxygen ($\delta^{18}O > 8.7$ ‰) comprise 78 % of samples from Jagersfontein, Juina, and Collier, but never found among Cullinan majorites (Fig. 3). Moreover, three Cullinan samples with the lowest $\delta^{18}O$ of 6.0, 6.6, and 7.0 ‰ are not matched by majorites from other locations (Fig. 3 and Table S-5). Majorite DIs from elsewhere may have formed from heavier, hydrothermally altered O source and were found in diamonds with the lighter $\delta^{13}C$ signatures sourced from organic matter or altered oceanic crust (−26 to −9 ‰, Fig. 3). In contrast, Cullinan majorite inclusions have been captured by diamonds with the mantle $\delta^{13}C$ signatures (−4.7 to −2.1 ‰, Fig. 3 and Table S-5). This pattern suggests an exclusively shallow crustal source of C and O for majorite-bearing diamonds from Jagersfontein, Juina, and Collier, while the oxygen isotope composition of Cullinan majorites possesses crustal signatures, and host diamonds show prominent affinity with mantle source of carbon. Diamond formation processes in the majorite-hosting diamonds locations were clearly different even though all the majorites formed in the deeply subducted mafic slab and had low-Cr eclogitic major element compositions.

Statistical t-test for $\delta^{18}O$ in Garnets from Diamondiferous and Barren Eclogites from the Kaapvaal Craton

We carried out the independent two-sample unequal *t*-test for the diamondiferous and barren eclogites from the Kaapvaal craton (Table S-2). The *t*-test determines that the average $\delta^{18}O$ and its distribution in garnet from the diamondiferous eclogites are distinct from the barren eclogites from the Kaapvaal craton with a probability >99.99 % (Table S-2).

Table S-2 Comparison of the garnet oxygen isotope composition ($\delta^{18}O$ in ‰) in the statistical samples of diamondiferous and barren eclogites from the Kaapvaal craton (data set: full list of references is given below).

Number of samples	**$\delta^{18}O$ in garnet Diamondiferous eclogites 42**	**$\delta^{18}O$ in garnet Barren eclogites 187**
Average $\delta^{18}O$ (in ‰)	7.28	5.04
1σ	1.31	1.49
t-test (calc.)		9.77
Significance level:		
0.01 %		4.13
0.1 %		3.44
1 %		2.65

Geochemical Modelling of $\delta^{18}O$ and $\delta^{13}C$ Effects of Decarbonation Reactions

Numerical modelling of decarbonation at temperatures 1000 and 1200 °C was carried out for the following reactions also listed in Table S-4:

1. $Alm + 3{\cdot}Mgs = Prp + Mag + 3{\cdot}C + 2.5{\cdot}O_2$
2. $2{\cdot}Grt + 2{\cdot}Ttn + 2{\cdot}Mgs = 2{\cdot}Grt + Cpx + 2{\cdot}Ilm + 2{\cdot}C + 2{\cdot}O_2$
3. $2{\cdot}Grt + 2{\cdot}Ttn + 2{\cdot}Mgs = 2{\cdot}Grt + Cpx + 2{\cdot}Ilm + 2{\cdot}CO_2$
4. $Prp + Rt + Mgs = Mg\text{-}Prp + Gk + CO_2$
5. $Prp + 2{\cdot}Qz + Dol = Prp + Di + 2{\cdot}CO_2$
6. $3{\cdot}Prp + 4{\cdot}Qz + 2{\cdot}Mgs = 2{\cdot}Prp + 4{\cdot}En + 2{\cdot}Ky + 2{\cdot}CO_2$
7. $Grs + Di + 2{\cdot}Qz + Dol = Grs + 2{\cdot}Di + 2{\cdot}CO_2$

All phases except O_2 in the proposed reactions are found in cratonic eclogites (*e.g.*, Jacob, 2004; Smith *et al.*, 2015; Mikhailenko *et al.*, 2022), and some of them are one of several end members of more complex mineral composition (Di and En as a component of omphacite eclogitic Cpx; Alm, Grs, and Prp are components of a more complex Grt composition). Quartz substitutes for coesite for the purpose of $\delta^{18}O$ modelling. As can be seen from reactions 1 and 2 above, they produce O_2, which we treat as a virtual component, not as a free gas phase in the deep mantle. The oxygen oxidises garnet and clinopyroxene, for example in reaction (8a):

8a. $\mathbf{2}{\cdot}(Fe^{2+}_{2.13}Mg_{0.62}Ca_{0.25})_{3.00}\,Al_{2.00}\,[SiO_4]_3 + \mathbf{8}{\cdot}(Ca_{0.20}Na_{0.80})_{1.00}(Mg_{0.20}Al_{0.80})_{1.00}\,(Si_2O_6) + \mathbf{5.5}{\cdot}(Ca_{0.90}Na_{0.10})_{1.00}\,(Mg_{0.82}Fe^{2+}_{0.08}Al_{0.10})_{1.00}\,(Si_2O_6) + \mathbf{0.5}{\cdot}O_2$

=

$\mathbf{3}{\cdot}(Mg_{1.10}Ca_{1.00}Fe^{2+}_{0.90})_{3.00}\,(Al_{1.98}Fe^{3+}_{0.02})_{2.00}\,[SiO_4]_3 + \mathbf{10}{\cdot}(Ca_{0.35}\,Na_{0.65})_{1.00}\,(Mg_{0.35}\,Al_{0.46}\,Fe^{3+}_{0.19})_{1.00}\,(Si_2O_6) + (Ca_{0.55}\,Na_{0.45})_{1.00}\,(Mg_{0.55}\,Al_{0.41}\,Fe^{3+}_{0.04})_{1.00}\,(Si_2O_6) + \mathbf{2}{\cdot}SiO_2.$

Compositions of garnet and clinopyroxene in the reaction are taken from natural eclogite samples where mineral Fe^{3+} are analysed (Kopylova *et al.*, 2016; Aulbach *et al.*, 2022). For the purposes of oxygen isotope modelling, the reaction is simplified as:

8b. $2{\cdot}Grt + 13.5{\cdot}Cpx + 0.5{\cdot}O_2 = 3{\cdot}Grt + 11{\cdot}Cpx + 2{\cdot}Qz(Coe).$

Reactions (1–8) are fully balanced. We assumed the initial equilibrium of all reactants with garnet with $\delta^{18}O = +6$ ‰. The modelling used oxygen and carbon fractionation factors derived from isotope equilibration of silicate minerals with carbonate, of CO_2 and O_2 and applicable to high temperatures of the lithospheric mantle (Table S-3). We also calculated relevant oxygen isotope fractionation factors (Table S-3) from the internally consistent database of Vho *et al.* (2019) at 1000 and 1200 °C. For reaction 8 that involves oxidation, we used O_2 with a range of $\delta^{18}O$ values calculated from reactions (1) and (2); net effects for combined reactions (1) + (8) and (2) + (8) are also listed (Table S-4).

Table S-3 Fractionation of oxygen isotopes in the modelled decarbonation reactions at 1000 and 1200 °C

Reaction	$10^3 \ln\alpha$ at 1000 °C	$10^3 \ln\alpha$ at 1200 °C	References
Alm–Mag	2.23	1.85	Calculated from database of Vho *et al.* (2019)
Alm–Mgs	−2.28	−1.91	Calculated from database of Vho *et al.* (2019)
Grs–Di	−0.34	−0.27	Calculated from database of Vho *et al.* (2019)
Grs–Dol	−2.36	−1.96	Calculated from database of Vho *et al.* (2019)
Grs–Qz	−2.35	−1.93	Calculated from database of Vho *et al.* (2019)
Grt–Cpx	0.02	0.02	Chacko *et al.* (2001)
Grt–Mag	2.21	1.65	Chacko *et al.* (2001)
Grt–Ttn	0.59	0.44	Chacko *et al.* (2001)
Jd–Prp	1.36	1.14	Calculated from database of Vho *et al.* (2019)
Jd–Qz(Coe)	−1.24	−1.03	Calculated from database of Vho *et al.* (2019)
Mgs–CO_2	1.86	1.43	Chacko and Deines (2008)
Prp–Dol	−2.62	−2.20	Calculated from database of Vho *et al.* (2019)
Prp–En	−0.39	−0.31	Calculated from database of Vho *et al.* (2019)
Prp–Gk	2.39	1.98	Calculated from database of Vho *et al.* (2019)
Prp–Ilm	2.13	1.76	Calculated from database of Vho *et al.* (2019)
Prp–Jd	−1.36	−1.14	Calculated from database of Vho *et al.* (2019)
Prp–Ky	0.89	0.71	Calculated from database of Vho *et al.* (2019)
Prp–Mgs	−2.54	−2.13	Calculated from database of Vho *et al.* (2019)
Prp–Qz	−2.61	−2.17	Calculated from database of Vho *et al.* (2019)
Prp–Rt	1.21	1.02	Calculated from database of Vho *et al.* (2019)
Prp–Ttn	−0.06	−0.04	Calculated from database of Vho *et al.* (2019)
Qz–Dol	−0.02	−0.03	Calculated from database of Vho *et al.* (2019)
Qz–Mgs	−0.02	−0.03	Calculated from database of Vho *et al.* (2019)

Mineral abbreviations (according to Warr, 2021): Alm, Almandine; Coe, coesite; Cpx, clinopyroxene; Di, diopside; Dol, dolomite; En, enstatite; Gk, geikielite; Grs, grossular; Grt, garnet; Ilm, ilmenite; Jd, jadeite; Ky, kyanite; Mag, magnetite; Mgs, magnesite; Prp, pyrope; Rt, rutile; Qz, quartz; Ttn, titanite.

Table S-4 $\delta^{18}O$ effects for reactions of diamond formation

Reaction #	Reactions	$\delta^{18}O$ effect on the resulting Grt (‰) as the reaction proceeds	
		at 1000 °C	at 1200 °C
1	Alm + 3·Mgs = Prp + Mag + 3·C + 2.5·O_2	1.3–1.4	1.0–1.1
2	2·Grt + 2·Ttn + 2·Mgs = 2·Grt + Cpx + 2·Ilm + 2·C + 2·O_2	0.6	0.5
3	2·Grt + 2·Ttn + 2·Mgs = 2·Grt + Cpx + 2·Ilm + 2·CO_2	0.1–0.3	0.1–0.3
4	Prp + Rt + Mgs = Mg-Prp + Gk + CO_2	0.03–0.2	0.1–0.2
5	Prp + 2·Qz +Dol = Prp + Di + 2·CO_2	0.1–0.5	0.2–0.4
6	3·Prp + 4·Qz + 2·Mgs = 2·Prp + 4·En + 2·Ky + 2·CO_2	0.5–0.6	0.5
7	Grs + Di + 2·Qz + Dol = Grs + 2·Di + 2·CO_2	−1.6 to −1.4	−1.6 to −1.4
8	2·Grt + 13.5·Cpx + 0.5·O_2 = 3·Grt + 11·Cpx + 2·Qz(Coe)	0.1	0.1
(1) + (8)	Net effect for (8) taking place after (1)	1.4–1.5	1.1–1.2
(2) + (8)	Net effect for (8) taking place after (2)	0.7	0.6

Calculations are done for $\delta^{18}O$ of the Grt/Alm reactant of 6 ‰ and $\delta^{13}C$ of Mgs reactant of −6 ‰. Abbreviations of minerals (according to Warr, 2021): Alm, almandine; Cpx, clinopyroxene; Di, diopside; Dol, dolomite; En, enstatite; Gk, geikielite; Grs, grossular; Grt, garnet; Ilm, ilmenite; Jd, jadeite; Ky, kyanite; Mag, magnetite; Mgs, magnesite; Prp, pyrope; Rt, rutile; Qz, quartz; Ttn, titanite.

The decarbonation was considered as a Rayleigh process in accordance with (Baumgartner and Valley, 2001), where the O isotope composition of the metasomatic agent is described as:

$$\delta_{Mgs} = 10^3[f^{\alpha-1} - 1] \quad \text{(Eq. S-2)}$$

where δ_{Mgs} – oxygen isotope composition of magnesite at any stage of the decarbonation; f – the extent to which the decarbonation reaction proceeds, or an abundance of oxygen in the carbonate residue; α – the fractionation coefficient of oxygen isotopes in the CO_2-Mgs (O_2-Mgs) system.

For any state of the system characterised by value f, the following equation calculates $\delta^{18}O$ of CO_2 or O_2:

$$\delta_{\text{fluid}} = (\delta^0_{\text{Mgs}} - f \cdot \delta_{\text{Mgs}})/(1-f) \quad \text{(Eq. S-3)}$$

The oxygen isotope composition of the reaction products (for example, newly formed garnet and magnetite in Reaction 1) can be calculated using mass balance:

$$\delta_{\text{Prp}} = \frac{\delta_{\text{tot}} - \delta_{O_2} \cdot X_{O_2} + \Delta_{(\text{Grt}-\text{Mag})} \cdot X_{\text{Mag}}}{X_{\text{Grt}} + X_{\text{Mag}}} \quad \text{(Eq. S-4)}$$

where δ_{Prp} – oxygen isotope composition of the newly-formed pyrope; δ_{O2} – oxygen isotope composition of the product fluid phase; $\Delta_{Grt\text{-}Mag}$ – equilibrium oxygen isotope fractionation between garnet and magnetite; X_{O2}, X_{Grt}, and X_{Mag} – molar fractions of the reaction products oxygen, garnet, and magnetite, respectively; δ_{tot} – oxygen isotope composition of the whole (total) system.

All of the above reactions are applicable to majorite formation in the sublithospheric mantle. Carbonatitic fluids traverse the transition zone and the lower mantle (Collerson *et al.*, 2010; Timmerman *et al.*, 2021) as evidenced by micron-sized carbonate inclusions in sublithospheric diamonds (Kaminsky *et al.*, 2016; Zedgenizov *et al.*, 2016). Clinopyroxene (diopside) is stable in the transition zone to depths of ~570 km (17–18 GPa; Canil, 1994), while ilmenite is stable down to 20–26 GPa, at pressures of the lower mantle (Yu *et al.*, 2011). Ilmenite and magnetite are described as inclusions in sublithospheric diamonds (*e.g.*, Kaminsky *et al.*, 2001, 2009; Kaminsky, 2012). Titanite's *P-T* stability field as an independent phase and as a solid solution end member extends to the sublithospheric mantle as shown by experiments in the bulk mafic composition (Kanzaki *et al.*, 1991; Gasparik *et al.*, 1994; Knoche *et al.*, 1998). Coesite (quartz in the reactions from Table S-4) can be in equilibrium with majorite in the sublithospheric mantle down to about 10.5 GPa, subsequently in the transition zone it transforms into stishovite (Zhang *et al.*, 1996 and references therein). In the absence of fractionation coefficients for isotopes in majorite, we employed respective coefficients Δ_{Grt} for garnet.

Supplementary Table

Table S-5 (Sheet 1) Point-by-point data on oxygen isotope analyses of majorite and garnet inclusions from the Cullinan diamonds measured by SIMS. (Sheet 2) Averaged oxygen isotope and major-element composition (for samples) of majorite and garnet inclusions from the Cullinan diamonds measured by SIMS. (Sheet 3) Averaged major-element composition of the clinopyroxene inclusions from the studied Cullinan diamonds (in wt. %)

Table S-5 (.xlsx) is available for download from the online version of this article at https://doi.org/10.7185/geochemlet.2328.

References for Figures 1, S-3 and S-4, and Table S-2

The following references were used for compiling Figures 1a and S-3 and Table S-2.

Cullinan (Premier) diamond inclusions (50 samples)

This study

Kaapvaal barren eclogites (187 samples)

Aulbach, S., Viljoen, K.S. (2015) Eclogite xenoliths from the Lace kimberlite, Kaapvaal craton: from convecting mantle source to palaeo-ocean floor and back. *Earth and Planetary Science Letters* 431, 274–286. https://doi.org/10.1016/j.epsl.2015.08.039

Aulbach, S., Gerdes, A., Viljoen, K.S. (2016) Formation of diamondiferous kyanite–eclogite in a subduction mélange. *Geochimica et Cosmochimica Acta* 179, 156–176. https://doi.org/10.1016/j.gca.2016.01.038

Aulbach, S., Woodland, A.B., Vasilyev, P., Galvez, M.E., Viljoen, K.S. (2017) Effects of low-pressure igneous processes and subduction on $Fe^{3+}/\Sigma Fe$ and redox state of mantle eclogites from Lace (Kaapvaal craton). *Earth and Planetary Science Letters* 474, 283–295. https://doi.org/10.1016/j.epsl.2017.06.030

Aulbach, S., Woodland, A.B., Stern, R.A., Vasilyev, P., Heaman, L.M., Viljoen, K.S. (2019) Evidence for a dominantly reducing Archaean ambient mantle from two redox proxies, and low oxygen fugacity of deeply subducted oceanic crust. *Scientific Reports* 9, 20190. https://doi.org/10.1038/s41598-019-55743-1

Caporuscio, F.A. (1990) Oxygen isotope systematics of eclogite mineral phases from South Africa. *Lithos* 25, 203–210. https://doi.org/10.1016/0024-4937(90)90015-S

Caporuscio, F.A., Smyth, J.R. (1990) Trace element crystal chemistry of mantle eclogites. *Contributions to Mineralogy and Petrology* 105, 550–561. https://doi.org/10.1007/BF00302494

Garlick, G.D., MacGregor, I.D., Vogel, D.E. (1971) Oxygen Isotope Ratios in Eclogites from Kimberlites. *Science* 172, 1025–1027. https://doi.org/10.1126/science.172.3987.1025

Gréau, Y., Huang, J.X., Griffin, W.L., Renac, C., Alard, O., O'Reilly, S.Y. (2011) Type I eclogites from Roberts Victor kimberlites: Products of extensive mantle metasomatism. *Geochimica et Cosmochimica Acta* 75, 6927–6954. https://doi.org/10.1016/j.gca.2011.08.035

Hardman, M.F., Stachel, T., Pearson, D.G., Cano, E.J., Stern, R.A., Sharp, Z.D. (2021) Characterising the Distinct Crustal Protoliths of Roberts Victor Type I and II Eclogites. *Journal of Petrology* 62, egab090. https://doi.org/10.1093/petrology/egab090

Huang, J.-X., Gréau, Y., Griffin, W.L., O'Reilly, S.Y., Pearson, N.J. (2012) Multi-stage origin of Roberts Victor eclogites: Progressive metasomatism and its isotopic effects. *Lithos* 142–143, 161–181. https://doi.org/10.1016/j.lithos.2012.03.002

Huang, J.-X., Xiang, Y., An, Y., Griffin, W.L., Gréau, Y., Xie, L., Pearson, N.J., Yu, H., O'Reilly, S.Y. (2016) Magnesium and oxygen isotopes in Roberts Victor eclogites. *Chemical Geology* 438, 73–83. https://doi.org/10.1016/j.chemgeo.2016.05.030

Jacob, D.E., Bizimis, M., Salters, V.J.M. (2005) Lu–Hf and geochemical systematics of recycled ancient oceanic crust: evidence from Roberts Victor eclogites. *Contributions to Mineralogy and Petrology* 148, 707–720. https://doi.org/10.1007/s00410-004-0631-x

Jacob, D.E., Viljoen, K.S., Grassineau, N.V. (2009) Eclogite xenoliths from Kimberley, South Africa — A case study of mantle metasomatism in eclogites. *Lithos* 112 Supplement 2, 1002–1013. https://doi.org/10.1016/j.lithos.2009.03.034

Jagoutz, E., Dawson, J.B., Hoernes, S., Spettel, B., Wanke, H. (1984) Anorthositic oceanic crust in the Archean Earth. *Lunar and Planetary Science XV* Abstract, 395–396. https://articles.adsabs.harvard.edu//full/1984LPI....15..395J/0000395.000.html

Lowry, D., Mattey, D.P., Harris, J.W. (1999) Oxygen isotope composition of syngenetic inclusions in diamond from the Finsch Mine, RSA. *Geochimica et Cosmochimica Acta* 63, 1825–1836. https://doi.org/10.1016/S0016-7037(99)00120-9

MacGregor, I.D., Manton, W.I. (1986) Roberts Victor eclogites: Ancient oceanic crust. *Journal of Geophysical Research: Solid Earth* 91, 14063–14079. https://doi.org/10.1029/JB091iB14p14063

Neal, C.R., Taylor, L.A., Davidson, J.P., Holden, P., Halliday, A.N., Nixon, P.H., Paces, J.B., Clayton, R.N., Mayeda, T.K. (1990) Eclogites with oceanic crustal and mantle signatures from the Bellsbank kimberlite, South Africa, part 2: Sr, Nd, and O isotope geochemistry. *Earth and Planetary Science Letters* 99, 362–379. https://doi.org/10.1016/0012-821X(90)90140-S

Ongley, J.S., Basu, A.R., Kyser, T.K. (1987) Oxygen isotopes in coexisting garnets, clinopyroxenes and phlogopites of Roberts Victor eclogites: implications for petrogenesis and mantle metasomatism. *Earth and Planetary Science Letters* 83, 80–84. https://doi.org/10.1016/0012-821X(87)90052-5

Radu, I.-B., Harris, C., Moine, B.N., Costin, G., Cottin, J.-Y. (2019) Subduction relics in the subcontinental lithospheric mantle evidence from variation in the $\delta^{18}O$ value of eclogite xenoliths from the Kaapvaal craton. *Contributions to Mineralogy and Petrology* 174, 19. https://doi.org/10.1007/s00410-019-1552-z

Riches, A.J.V., Ickert, R.B., Pearson, D.G., Stern, R.A., Jackson, S.E., Ishikawa, A., Kjarsgaard, B.A., Gurney, J.J. (2016) *In situ* oxygen-isotope, major-, and trace-element constraints on the metasomatic modification and crustal origin of a diamondiferous eclogite from Roberts Victor, Kaapvaal Craton. *Geochimica et Cosmochimica Acta* 174, 345–359. https://doi.org/10.1016/j.gca.2015.11.028

Schulze, D.J., Valley, J.W., Spicuzza, M.J. (2000) Coesite eclogites from the Roberts Victor kimberlite, South Africa. *Lithos* 54, 23–32. https://doi.org/10.1016/S0024-4937(00)00031-1

Shervais, J.W., Taylor, L.A., Lugmair, G.W., Clayton, R.N., Mayeda, T.K., Korotev, R.L. (1988) Early Proterozoic oceanic crust and the evolution of subcontinental mantle: Eclogites and related rocks from southern Africa. *GSA Bulletin* 100, 411–423. https://doi.org/10.1130/0016-7606(1988)100<0411:EPOCAT>2.3.CO;2

Shu, Q., Brey, G.P., Hoefer, H.E., Zhao, Z., Pearson, D.G. (2016) Kyanite/corundum eclogites from the Kaapvaal Craton: subducted troctolites and layered gabbros from the Mid- to Early Archean. *Contributions to Mineralogy and Petrology* 171, 11. https://doi.org/10.1007/s00410-015-1225-5

Taylor, L.A., Neal, C.R. (1989) Eclogites with Oceanic Crustal and Mantle Signatures from the Bellsbank Kimberlite, South Africa, Part I: Mineralogy, Petrography, and Whole Rock Chemistry. *The Journal of Geology* 97, 551–567. https://doi.org/10.1086/629334

Viljoen, K.S., Schulze, D.J., Quadling, A.G. (2005) Contrasting Group I and Group II Eclogite Xenolith Petrogenesis: Petrological, Trace Element and Isotopic Evidence from Eclogite, Garnet-Websterite and Alkremite Xenoliths in the Kaalvallei Kimberlite, South Africa. *Journal of Petrology* 46, 2059–2090. https://doi.org/10.1093/petrology/egi047

The following references were used for compiling Figures 1b and S-4 and Table S-2.

Diamondiferous eclogites worldwide (210 samples)

Aulbach, S., Jacob, D.E., Cartigny, P., Stern, R.A., Simonetti, S.S., Wörner, G., Viljoen, K.S. (2017) Eclogite xenoliths from Orapa: Ocean crust recycling, mantle metasomatism and carbon cycling at the western Zimbabwe craton margin. *Geochimica et Cosmochimica Acta* 213, 574–592. https://doi.org/10.1016/j.gca.2017.06.038

Aulbach, S., Woodland, A.B., Stern, R.A., Vasilyev, P., Heaman, L.M., Viljoen, K.S. (2019) Evidence for a dominantly reducing Archaean ambient mantle from two redox proxies, and low oxygen fugacity of deeply subducted oceanic crust. *Scientific Reports* 9, 20190. https://doi.org/10.1038/s41598-019-55743-1

Beard, B.L., Fraracci, K.N., Clayton, R.A., Mayeda, T.K., Snyder, G.A., Sobolev, N.V., Taylor, L.A. (1996) Petrography and geochemistry of eclogites from the Mir kimberlite, Yakutia, Russia. *Contributions to Mineralogy and Petrology* 125, 293–310. https://doi.org/10.1007/s004100050223

Carmody, L., Barry, P.H., Shervais, J.W., Kluesner, J.W., Taylor, L.A. (2013) Oxygen isotopes in subducted oceanic crust: A new perspective from Siberian diamondiferous eclogites. *Geochemistry, Geophysics, Geosystems* 14, 3479–3493. https://doi.org/10.1002/ggge.20220

Deines, P., Harris, J.W., Robinson, D.N., Gurney, J.J., Shee, S.R. (1991) Carbon and oxygen isotope variations in diamond and graphite eclogites from Orapa, Botswana, and the nitrogen content of their diamonds. *Geochimica et Cosmochimica Acta* 55, 515–524. https://doi.org/10.1016/0016-7037(91)90009-T

Jacob, D.E., Foley, S.F. (1999) Evidence for Archean ocean crust with low high field strength element signature from diamondiferous eclogite xenoliths. *Lithos* 48, 317–336. https://doi.org/10.1016/S0024-4937(99)00034-1

Jacob, D., Jagoutz, E., Lowry, D., Mattey, D., Kudrjavtseva, G. (1994) Diamondiferous eclogites from Siberia: Remnants of Archean oceanic crust. *Geochimica et Cosmochimica Acta* 58, 5191–5207. https://doi.org/10.1016/0016-7037(94)90304-2

Jerde, E.A., Taylor, L.A., Crozaz, G., Sobolev, N.V., Sobolev, V.N. (1993) Diamondiferous eclogites from Yakutia, Siberia: evidence for a diversity of protoliths. *Contributions to Mineralogy and Petrology* 114, 189–202. https://doi.org/10.1007/BF00307755

Liu, Y., Taylor, L.A., Sarbadhikari, A.B., Valley, J.W., Ushikubo, T., Spicuzza, M.J., Kita, N., Ketcham, R.A., Carlson, W., Shatsky, V. (2009) Metasomatic origin of diamonds in the world's largest diamondiferous eclogite. *Lithos* 112 Supplement 2, 1014–1024. https://doi.org/10.1016/j.lithos.2009.06.036

Pernet-Fisher, J.F., Howarth, G.H., Liu, Y., Barry, P.H., Carmody, L., Valley, J.W., Bodnar, R.J., Spetsius, Z.V., Taylor, L.A. (2014) Komsomolskaya diamondiferous eclogites: evidence for oceanic crustal protoliths. *Contributions to Mineralogy and Petrology* 167, 981. https://doi.org/10.1007/s00410-014-0981-y

Riches, A.J.V., Liu, Y., Day, J.M.D., Spetsius, Z.V., Taylor, L.A. (2010) Subducted oceanic crust as diamond hosts revealed by garnets of mantle xenoliths from Nyurbinskaya, Siberia. *Lithos* 120, 368–378. https://doi.org/10.1016/j.lithos.2010.09.006

Riches, A.J.V., Ickert, R.B., Pearson, D.G., Stern, R.A., Jackson, S.E., Ishikawa, A., Kjarsgaard, B.A., Gurney, J.J. (2016) *In situ* oxygen-isotope, major-, and trace-element constraints on the metasomatic modification and crustal origin of a diamondiferous eclogite from Roberts Victor, Kaapvaal Craton. *Geochimica et Cosmochimica Acta* 174, 345–359. https://doi.org/10.1016/j.gca.2015.11.028

Robinson, D.M., Gurney, J.J., Shee, S.R. (1984) Diamond eclogite and graphite eclogite xenoliths from Orapa, Botswana. In: Kornprobst, J. (Ed.) *Kimberlites II: The Mantle and Crust-Mantle Relationships*, Developments in Petrology 11, Elsevier, Amsterdam, 11–24. https://doi.org/10.1016/B978-0-444-42274-3.50008-1

Shatsky, V.S., Zedgenizov, D.A., Ragozin, A.L. (2016) Evidence for a subduction component in the diamond-bearing mantle of the Siberian craton. *Russian Geology and Geophysics* 57, 111–126. https://doi.org/10.1016/j.rgg.2016.01.008

Smart, K.A., Chacko, T., Stachel, T., Tappe, S., Stern, R.A., Ickert, R.B., EIMF (2012) Eclogite formation beneath the northern Slave craton constrained by diamond inclusions: Oceanic lithosphere origin without a crustal signature. *Earth and Planetary Science Letters* 319–320, 165–177. https://doi.org/10.1016/j.epsl.2011.12.032

Smart, K.A., Chacko, T., Simonetti, A., Sharp, Z.D., Heaman, L.M. (2014) A Record of Paleoproterozoic Subduction Preserved in the Northern Slave Cratonic Mantle: Sr–Pb–O Isotope and Trace-element Investigations of Eclogite Xenoliths from the Jericho and Muskox Kimberlites. *Journal of Petrology* 55, 549–583. https://doi.org/10.1093/petrology/egt077

Smyth, J.R., Caporuscio, F.A., McCormick, T.C. (1989) Mantle eclogites: evidence of igneous fractionation in the mantle. *Earth and Planetary Science Letters* 93, 133–141. https://doi.org/10.1016/0012-821X(89)90191-X

Snyder, G.A., Jerde, E.A., Taylor, L.A., Halliday, A.N., Sobolev, V.N., Sobolev, N.V. (1993) Nd and Sr isotopes from diamondiferous eclogites, Udachnaya Kimberlite Pipe, Yakutia, Siberia: Evidence of differentiation in the early Earth? *Earth and Planetary Science Letters* 118, 91–100. https://doi.org/10.1016/0012-821X(93)90161-2

Snyder, G.A., Taylor, L.A., Jerde, E.A., Clayton, R.N., Mayeda, T.K., Deines, P., Rossman, G.R., Sobolev, N.V. (1995) Archean mantle heterogeneity and the origin of diamondiferous eclogites, Siberia: Evidence from stable isotopes and hydroxyl in garnet. *American Mineralogist* 80, 799–809. https://doi.org/10.2138/am-1995-7-816

Snyder, G.A., Taylor, L.A., Grozaz, G., Halliday, A.N., Beard, B.L., Sobolev, V.N., Sobolev, N.V. (1997) The Origins of Yakutian Eclogite Xenoliths. *Journal of Petrology* 38, 85–113. https://doi.org/10.1093/petroj/38.1.85

Spetsius, Z.V., Taylor, L.A., Valley, J.W., Deangelis, M.T., Spicuzza, M., Ivanov, A.S., Banzeruk, V.I. (2008) Diamondiferous xenoliths from crustal subduction: garnet oxygen isotopes from the Nyurbinskaya pipe, Yakutia. *European Journal of Mineralogy* 20, 375–385. https://doi.org/10.1127/0935-1221/2008/0020-1828

Ukhanov, A.V., Ryabchikov, I.D., Khar'kiv, A.D. (1988) *Lithospheric mantle of the Yakutian kimberlite province*. Publishing House "Nauka", Moscow.

Ustinov, V.I., Ukhanov, V.A., Grinenko, V.A., Gavrilov, Y.Y. (1987) $\delta^{18}O$ in eclogites from the Udachnaya and Obnazhennaya kimberlites pipes. *Geokhimiya* 11, 1637–1641. (in Russian)

Viljoen, K.S., Schulze, D.J., Quadling, A.G. (2005) Contrasting Group I and Group II Eclogite Xenolith Petrogenesis: Petrological, Trace Element and Isotopic Evidence from Eclogite, Garnet-Websterite and Alkremite Xenoliths in the Kaalvallei Kimberlite, South Africa. *Journal of Petrology* 46, 2059–2090. https://doi.org/10.1093/petrology/egi047

Zedgenizov, D.A., Ragozin, A.L., Shatsky, V.S. (2007) Chloride-carbonate fluid in diamonds from the eclogite xenolith. *Doklady Earth Sciences* 415, 961–964. https://doi.org/10.1134/S1028334X07060293

Garnet diamond inclusions worldwide (89 samples)

Anand, M., Taylor, L.A., Misra, K.C., Carlson, W.D., Sobolev, N.V. (2004) Nature of diamonds in Yakutian eclogites: views from eclogite tomography and mineral inclusions in diamonds. *Lithos* 77, 333–348. https://doi.org/10.1016/j.lithos.2004.03.026

Burnham, A.D., Thomson, A.R., Bulanova, G.P., Kohn, S.C., Smith, C.B., Walter, M.J. (2015) Stable isotope evidence for crustal recycling as recorded by superdeep diamonds. *Earth and Planetary Science Letters* 432, 374–380. https://doi.org/10.1016/j.epsl.2015.10.023

Ickert, R.B., Stachel, T., Stern, R.A., Harris, J.W. (2013) Diamond from recycled crustal carbon documented by coupled $\delta^{18}O$–$\delta^{13}C$ measurements of diamonds and their inclusions. *Earth and Planetary Science Letters* 364, 85–97. https://doi.org/10.1016/j.epsl.2013.01.008

Ickert, R.B., Stachel, T., Stern, R.A., Harris, J.W. (2015) Extreme ^{18}O-enrichment in majorite constrains a crustal origin of transition zone diamonds. *Geochemical Perspectives Letters* 1, 65–74. https://doi.org/10.7185/geochemlet.1507

Lowry, D., Mattey, D.P., Harris, J.W. (1999) Oxygen isotope composition of syngenetic inclusions in diamond from the Finsch Mine, RSA. *Geochimica et Cosmochimica Acta* 63, 1825–1836. https://doi.org/10.1016/S0016-7037(99)00120-9

Schulze, D.J., Harte, B., Edinburgh Ion Microprobe Facility staff, Page, F.Z., Valley, J.W., Channer, D.M.D., Jaques, A.L. (2013) Anticorrelation between low $\delta^{13}C$ of eclogitic diamonds and high $\delta^{18}O$ of their coesite and garnet inclusions requires a subduction origin. *Geology* 41, 455–458. https://doi.org/10.1130/G33839.1

Smart, K.A., Chacko, T., Stachel, T., Tappe, S., Stern, R.A., Ickert, R.B., EIMF (2012) Eclogite formation beneath the northern Slave craton constrained by diamond inclusions: Oceanic lithosphere origin without a crustal signature. *Earth and Planetary Science Letters* 319–320, 165–177. https://doi.org/10.1016/j.epsl.2011.12.032

Zedgenizov, D., Rubatto, D., Shatsky, V., Ragozin, A., Kalinina, V. (2016) Eclogitic diamonds from variable crustal protoliths in the northeastern Siberian craton: Trace elements and coupled $\delta^{13}C$–$\delta^{18}O$ signatures in diamonds and garnet inclusions. *Chemical Geology* 422, 46–59. https://doi.org/10.1016/j.chemgeo.2015.12.018

References for Figure 2

The following references were used for compiling Figure 2.

Barren eclogites

Aulbach, S., Jacob, D.E., Cartigny, P., Stern, R.A., Simonetti, S.S., Wörner, G., Viljoen, K.S. (2017) Eclogite xenoliths from Orapa: Ocean crust recycling, mantle metasomatism and carbon cycling at the western Zimbabwe craton margin. *Geochimica et Cosmochimica Acta* 213, 574–592. https://doi.org/10.1016/j.gca.2017.06.038

Barth, M.G., Rudnick, R.L., Horn, I., McDonough, W.F., Spicuzza, M.J., Valley, J.W., Haggerty, S.E. (2001) Geochemistry of xenolithic eclogites from West Africa, part I: A link between low MgO eclogites and archean crust formation. *Geochimica et Cosmochimica Acta* 65, 1499–1527. https://doi.org/10.1016/S0016-7037(00)00626-8

Caporuscio, F.A. (1990) Oxygen isotope systematics of eclogite mineral phases from South Africa. *Lithos* 25, 203–210. https://doi.org/10.1016/0024-4937(90)90015-S

Caporuscio, F.A., Smyth, J.R. (1990) Trace element crystal chemistry of mantle eclogites. *Contributions to Mineralogy and Petrology* 105, 550–561. https://doi.org/10.1007/BF00302494

Fung, A.T., Haggerty, S.E. (1995) Petrography and mineral compositions of eclogites from the Koidu Kimberlite Complex, Sierra Leone. *Journal of Geophysical Research: Solid Earth* 100, 20451–20473. https://doi.org/10.1029/95JB01573

Garlick, G.D., MacGregor, I.D., Vogel, D.E. (1971) Oxygen Isotope Ratios in Eclogites from Kimberlites. *Science* 172, 1025–1027. https://doi.org/10.1126/science.172.3987.1025

Hardman, M.F., Stachel, T., Pearson, D.G., Cano, E.J., Stern, R.A., Sharp, Z.D. (2021) Characterising the Distinct Crustal Protoliths of Roberts Victor Type I and II Eclogites. *Journal of Petrology* 62, egab090. https://doi.org/10.1093/petrology/egab090

Hills, D.V., Haggerty, S.E. (1989) Petrochemistry of eclogites from the Koidu Kimberlite Complex, Sierra Leone. *Contributions to Mineralogy and Petrology* 103, 397–422. https://doi.org/10.1007/BF01041749

Jacob, D.E., Bizimis, M., Salters, V.J.M. (2005) Lu–Hf and geochemical systematics of recycled ancient oceanic crust: evidence from Roberts Victor eclogites. *Contributions to Mineralogy and Petrology* 148, 707–720. https://doi.org/10.1007/s00410-004-0631-x

Jacob, D.E., Viljoen, K.S., Grassineau, N.V. (2009) Eclogite xenoliths from Kimberley, South Africa — A case study of mantle metasomatism in eclogites. *Lithos* 112 Supplement 2, 1002–1013. https://doi.org/10.1016/j.lithos.2009.03.034

Jagoutz, E., Dawson, J.B., Hoernes, S., Spettel, B., Wanke, H. (1984) Anorthositic oceanic crust in the Archean Earth. *Lunar and Planetary Science XV* Abstract, 395–396. https://articles.adsabs.harvard.edu//full/1984LPI....15..395J/0000395.000.html

Korolev, N., Nikitina, L.P., Goncharov, A., Dubinina, E.O., Melnik, A., Müller, D., Chen, Y.-X., Zinchenko, V.N. (2021) Three Types of Mantle Eclogite from Two Layers of Oceanic Crust: A Key Case of Metasomatically-Aided Transformation of Low-to-High-Magnesian Eclogite. *Journal of Petrology* 62, egab070. https://doi.org/10.1093/petrology/egab070

Lowry, D., Mattey, D.P., Harris, J.W. (1999) Oxygen isotope composition of syngenetic inclusions in diamond from the Finsch Mine, RSA. *Geochimica et Cosmochimica Acta* 63, 1825–1836. https://doi.org/10.1016/S0016-7037(99)00120-9

MacGregor, I.D., Manton, W.I. (1986) Roberts Victor eclogites: Ancient oceanic crust. *Journal of Geophysical Research: Solid Earth* 91, 14063–14079. https://doi.org/10.1029/JB091iB14p14063

Neal, C.R., Taylor, L.A., Davidson, J.P., Holden, P., Halliday, A.N., Nixon, P.H., Paces, J.B., Clayton, R.N., Mayeda, T.K. (1990) Eclogites with oceanic crustal and mantle signatures from the Bellsbank kimberlite, South Africa, part 2: Sr, Nd, and O isotope geochemistry. *Earth and Planetary Science Letters* 99, 362–379. https://doi.org/10.1016/0012-821X(90)90140-S

Ongley, J.S., Basu, A.R., Kyser, T.K. (1987) Oxygen isotopes in coexisting garnets, clinopyroxenes and phlogopites of Roberts Victor eclogites: implications for petrogenesis and mantle metasomatism. *Earth and Planetary Science Letters* 83, 80–84. https://doi.org/10.1016/0012-821X(87)90052-5

Qi, Q., Taylor, L.A., Snyder, G.A., Clayton, R.N., Mayeda, T.K., Sobolev, N.V. (1997) Detailed petrology and geochemistry of a rare corundum eclogite xenolith from Obnazhennaya, Yakutia. *Russian Geology and Geophysics* 38, 247–260.

Radu, I.-B., Harris, C., Moine, B.N., Costin, G., Cottin, J.-Y. (2019) Subduction relics in the subcontinental lithospheric mantle evidence from variation in the $\delta^{18}O$ value of eclogite xenoliths from the Kaapvaal craton. *Contributions to Mineralogy and Petrology* 174, 19. https://doi.org/10.1007/s00410-019-1552-z

Riches, A.J.V., Ickert, R.B., Pearson, D.G., Stern, R.A., Jackson, S.E., Ishikawa, A., Kjarsgaard, B.A., Gurney, J.J. (2016) *In situ* oxygen-isotope, major-, and trace-element constraints on the metasomatic modification and crustal origin of a diamondiferous eclogite from Roberts Victor, Kaapvaal Craton. *Geochimica et Cosmochimica Acta* 174, 345–359. https://doi.org/10.1016/j.gca.2015.11.028

Robinson, D.M., Gurney, J.J., Shee, S.R. (1984) Diamond eclogite and graphite eclogite xenoliths from Orapa, Botswana. In: Kornprobst, J. (Ed.) *Kimberlites II: The Mantle and Crust-Mantle Relationships*, Developments in Petrology 11, Elsevier, Amsterdam, 11–24. https://doi.org/10.1016/B978-0-444-42274-3.50008-1

Schmidberger, S.S., Simonetti, A., Heaman, L.M., Creaser, R.A., Whiteford, S. (2007) Lu–Hf, in-situ Sr and Pb isotope and trace element systematics for mantle eclogites from the Diavik diamond mine: Evidence for Paleoproterozoic subduction beneath the Slave craton, Canada. *Earth and Planetary Science Letters* 254, 55–68. https://doi.org/10.1016/j.epsl.2006.11.020

Shervais, J.W., Taylor, L.A., Lugmair, G.W., Clayton, R.N., Mayeda, T.K., Korotev, R.L. (1988) Early Proterozoic oceanic crust and the evolution of subcontinental mantle: Eclogites and related rocks from southern Africa. *GSA Bulletin* 100, 411–423. https://doi.org/10.1130/0016-7606(1988)100<0411:EPOCAT>2.3.CO;2

Shu, Q., Brey, G.P., Hoefer, H.E., Zhao, Z., Pearson, D.G. (2016) Kyanite/corundum eclogites from the Kaapvaal Craton: subducted troctolites and layered gabbros from the Mid- to Early Archean. *Contributions to Mineralogy and Petrology* 171, 11. https://doi.org/10.1007/s00410-015-1225-5

Smyth, J.R., Caporuscio, F.A., McCormick, T.C. (1989) Mantle eclogites: evidence of igneous fractionation in the mantle. *Earth and Planetary Science Letters* 93, 133–141. https://doi.org/10.1016/0012-821X(89)90191-X

Taylor, L.A., Neal, C.R. (1989) Eclogites with Oceanic Crustal and Mantle Signatures from the Bellsbank Kimberlite, South Africa, Part I: Mineralogy, Petrography, and Whole Rock Chemistry. *The Journal of Geology* 97, 551–567. https://doi.org/10.1086/629334

Ukhanov, A.V., Ryabchikov, I.D., Khar'kiv, A.D. (1988) *Lithospheric mantle of the Yakutian kimberlite province*. Publishing House "Nauka", Moscow.

Ustinov, V.I., Ukhanov, V.A., Grinenko, V.A., Gavrilov, Y.Y. (1987) $\delta^{18}O$ in eclogites from the Udachnaya and Obnazhennaya kimberlites pipes. *Geokhimiya* 11, 1637–1641. (in Russian)

Viljoen, K.S., Smith, C.B., Sharp, Z.D. (1996) Stable and radiogenic isotope study of eclogite xenoliths from the Orapa kimberlite, Botswana. *Chemical Geology* 131, 235–255. https://doi.org/10.1016/0009-2541(96)00018-6

Viljoen, K.S., Schulze, D.J., Quadling, A.G. (2005) Contrasting Group I and Group II Eclogite Xenolith Petrogenesis: Petrological, Trace Element and Isotopic Evidence from Eclogite, Garnet-Websterite and Alkremite Xenoliths in the Kaalvallei Kimberlite, South Africa. *Journal of Petrology* 46, 2059–2090. https://doi.org/10.1093/petrology/egi047

Diamondiferous eclogites

Aulbach, S., Jacob, D.E., Cartigny, P., Stern, R.A., Simonetti, S.S., Wörner, G., Viljoen, K.S. (2017) Eclogite xenoliths from Orapa: Ocean crust recycling, mantle metasomatism and carbon cycling at the western Zimbabwe craton margin. *Geochimica et Cosmochimica Acta* 213, 574–592. https://doi.org/10.1016/j.gca.2017.06.038

Beard, B.L., Fraracci, K.N., Clayton, R.A., Mayeda, T.K., Snyder, G.A., Sobolev, N.V., Taylor, L.A. (1996) Petrography and geochemistry of eclogites from the Mir kimberlite, Yakutia, Russia. *Contributions to Mineralogy and Petrology* 125, 293–310. https://doi.org/10.1007/s004100050223

Deines, P., Harris, J.W., Robinson, D.N., Gurney, J.J., Shee, S.R. (1991) Carbon and oxygen isotope variations in diamond and graphite eclogites from Orapa, Botswana, and the nitrogen content of their diamonds. *Geochimica et Cosmochimica Acta* 55, 515–524. https://doi.org/10.1016/0016-7037(91)90009-T

Jacob, D.E., Foley, S.F. (1999) Evidence for Archean ocean crust with low high field strength element signature from diamondiferous eclogite xenoliths. *Lithos* 48, 317–336. https://doi.org/10.1016/S0024-4937(99)00034-1

Jacob, D., Jagoutz, E., Lowry, D., Mattey, D., Kudrjavtseva, G. (1994) Diamondiferous eclogites from Siberia: Remnants of Archean oceanic crust. *Geochimica et Cosmochimica Acta* 58, 5191–5207. https://doi.org/10.1016/0016-7037(94)90304-2

Jerde, E.A., Taylor, L.A., Crozaz, G., Sobolev, N.V., Sobolev, V.N. (1993) Diamondiferous eclogites from Yakutia, Siberia: evidence for a diversity of protoliths. *Contributions to Mineralogy and Petrology* 114, 189–202. https://doi.org/10.1007/BF00307755

Liu, Y., Taylor, L.A., Sarbadhikari, A.B., Valley, J.W., Ushikubo, T., Spicuzza, M.J., Kita, N., Ketcham, R.A., Carlson, W., Shatsky, V. (2009) Metasomatic origin of diamonds in the world's largest diamondiferous eclogite. *Lithos* 112 Supplement 2, 1014–1024. https://doi.org/10.1016/j.lithos.2009.06.036

Robinson, D.M., Gurney, J.J., Shee, S.R. (1984) Diamond eclogite and graphite eclogite xenoliths from Orapa, Botswana. In: Kornprobst, J. (Ed.) *Kimberlites II: The Mantle and Crust-Mantle Relationships*, Developments in Petrology 11, Elsevier, Amsterdam, 11–24. https://doi.org/10.1016/B978-0-444-42274-3.50008-1

Shatsky, V.S., Zedgenizov, D.A., Ragozin, A.L. (2016) Evidence for a subduction component in the diamond-bearing mantle of the Siberian craton. *Russian Geology and Geophysics* 57, 111–126. https://doi.org/10.1016/j.rgg.2016.01.008

Smart, K.A., Chacko, T., Stachel, T., Tappe, S., Stern, R.A., Ickert, R.B., EIMF (2012) Eclogite formation beneath the northern Slave craton constrained by diamond inclusions: Oceanic lithosphere origin without a crustal signature. *Earth and Planetary Science Letters* 319–320, 165–177. https://doi.org/10.1016/j.epsl.2011.12.032

Smart, K.A., Chacko, T., Simonetti, A., Sharp, Z.D., Heaman, L.M. (2014) A Record of Paleoproterozoic Subduction Preserved in the Northern Slave Cratonic Mantle: Sr–Pb–O Isotope and Trace-element Investigations of Eclogite Xenoliths from the Jericho and Muskox Kimberlites. *Journal of Petrology* 55, 549–583. https://doi.org/10.1093/petrology/egt077

Smyth, J.R., Caporuscio, F.A., McCormick, T.C. (1989) Mantle eclogites: evidence of igneous fractionation in the mantle. *Earth and Planetary Science Letters* 93, 133–141. https://doi.org/10.1016/0012-821X(89)90191-X

Snyder, G.A., Jerde, E.A., Taylor, L.A., Halliday, A.N., Sobolev, V.N., Sobolev, N.V. (1993) Nd and Sr isotopes from diamondiferous eclogites, Udachnaya Kimberlite Pipe, Yakutia, Siberia: Evidence of differentiation in the early Earth? *Earth and Planetary Science Letters* 118, 91–100. https://doi.org/10.1016/0012-821X(93)90161-2

Snyder, G.A., Taylor, L.A., Jerde, E.A., Clayton, R.N., Mayeda, T.K., Deines, P., Rossman, G.R., Sobolev, N.V. (1995) Archean mantle heterogeneity and the origin of diamondiferous eclogites, Siberia: Evidence from stable isotopes and hydroxyl in garnet. *American Mineralogist* 80, 799–809. https://doi.org/10.2138/am-1995-7-816

Snyder, G.A., Taylor, L.A., Grozaz, G., Halliday, A.N., Beard, B.L., Sobolev, V.N., Sobolev, N.V. (1997) The Origins of Yakutian Eclogite Xenoliths. *Journal of Petrology* 38, 85–113. https://doi.org/10.1093/petroj/38.1.85

Sobolev, V.N., Taylor, L.A., Snyder, G.A., Sobolev, N.V. (1994) Diamondiferous Eclogites from the Udachnaya Kimberlite Pipe, Yakutia. *International Geology Review* 36, 42–64. https://doi.org/10.1080/00206819409465448

Ukhanov, A.V., Ryabchikov, I.D., Khar'kiv, A.D. (1988) *Lithospheric mantle of the Yakutian kimberlite province*. Publishing House "Nauka", Moscow.

Ustinov, V.I., Ukhanov, V.A., Grinenko, V.A., Gavrilov, Y.Y. (1987) $\delta^{18}O$ in eclogites from the Udachnaya and Obnazhennaya kimberlites pipes. *Geokhimiya* 11, 1637–1641. (in Russian)

Viljoen, K.S., Schulze, D.J., Quadling, A.G. (2005) Contrasting Group I and Group II Eclogite Xenolith Petrogenesis: Petrological, Trace Element and Isotopic Evidence from Eclogite, Garnet-Websterite and Alkremite Xenoliths in the Kaalvallei Kimberlite, South Africa. *Journal of Petrology* 46, 2059–2090. https://doi.org/10.1093/petrology/egi047

Zedgenizov, D.A., Ragozin, A.L., Shatsky, V.S. (2007) Chloride–carbonate fluid in diamonds from the eclogite xenolith. *Doklady Earth Sciences* 415, 961–964. https://doi.org/10.1134/S1028334X07060293

Supplementary Information References

Arai, H. (2010) A function for the R programming language to recast garnet analyses into end-members: Revision and porting of Muhling and Griffin's method. *Computers & Geosciences* 36, 406–409. https://doi.org/10.1016/j.cageo.2009.05.007

Aulbach, S., Woodland, A.B., Vasilyev, P., Galvez, M.E., Viljoen, K.S. (2017) Effects of low-pressure igneous processes and subduction on $Fe^{3+}/\Sigma Fe$ and redox state of mantle eclogites from Lace (Kaapvaal craton). *Earth and Planetary Science Letters* 474, 283–295. https://doi.org/10.1016/j.epsl.2017.06.030

Aulbach, S., Woodland, A.B., Stagno, V., Korsakov, A.V., Mikhailenko, D., Golovin, A. (2022) Fe^{3+} Distribution and $Fe^{3+}/\Sigma Fe$-Oxygen Fugacity Variations in Kimberlite-Borne Eclogite Xenoliths, with Comments on Clinopyroxene-Garnet Oxy-Thermobarometry. *Journal of Petrology* 63, egac076. https://doi.org/10.1093/petrology/egac076

Baertschi, P. (1976) Absolute ^{18}O content of standard mean ocean water. *Earth and Planetary Science Letters* 31, 341–344. https://doi.org/10.1016/0012-821X(76)90115-1

Baumgartner, L.P., Valley, J.W. (2001) Stable Isotope Transport and Contact Metamorphic Fluid Flow. *Reviews in Mineralogy and Geochemistry* 43, 415–467. https://doi.org/10.2138/gsrmg.43.1.415

Burnham, A.D., Thomson, A.R., Bulanova, G.P., Kohn, S.C., Smith, C.B., Walter, M.J. (2015) Stable isotope evidence for crustal recycling as recorded by superdeep diamonds. *Earth and Planetary Science Letters* 432, 374–380. https://doi.org/10.1016/j.epsl.2015.10.023

Canil, D. (1994) Stability of clinopyroxene at pressure-temperature conditions of the transition region. *Physics of the Earth and Planetary Interiors* 86, 25–34. https://doi.org/10.1016/0031-9201(94)05059-7

Chacko, T., Deines, P. (2008) Theoretical calculation of oxygen isotope fractionation factors in carbonate systems. *Geochimica et Cosmochimica Acta* 72, 3642–3660. https://doi.org/10.1016/j.gca.2008.06.001

Chacko, T., Cole, D.R., Horita, J. (2001) Equilibrium Oxygen, Hydrogen and Carbon Isotope Fractionation Factors Applicable to Geologic Systems. *Reviews in Mineralogy and Geochemistry* 43, 1–81. https://doi.org/10.2138/gsrmg.43.1.1

Collerson, K.D., Williams, Q., Ewart, A.E., Murphy, D.T. (2010) Origin of HIMU and EM-1 domains sampled by ocean island basalts, kimberlites and carbonatites: The role of CO_2-fluxed lower mantle melting in thermochemical upwellings. *Physics of the Earth and Planetary Interiors* 181, 112–131. https://doi.org/10.1016/j.pepi.2010.05.008

Day, H.W. (2012) A revised diamond-graphite transition curve. *American Mineralogist* 97, 52–62. https://doi.org/10.2138/am.2011.3763

Deines, P., Harris, J.W., Robinson, D.N., Gurney, J.J., Shee, S.R. (1991) Carbon and oxygen isotope variations in diamond and graphite eclogites from Orapa, Botswana, and the nitrogen content of their diamonds. *Geochimica et Cosmochimica Acta* 55, 515–524. https://doi.org/10.1016/0016-7037(91)90009-T

Droop, G.T.R. (1987) A general equation for estimating Fe^{3+} concentrations in ferromagnesian silicates and oxides from microprobe analyses, using stoichiometric criteria. *Mineralogical Magazine* 51, 431–435. https://doi.org/10.1180/minmag.1987.051.361.10

Gasparik, T., Wolf, K., Smith, C.M. (1994) Experimental determination of phase relations in the $CaSiO_3$ system from 8 to 15 GPa. *American Mineralogist* 79, 1219–1222.

Hardman, M.F., Stachel, T., Pearson, D.G., Cano, E.J., Stern, R.A., Sharp, Z.D. (2021) Characterising the Distinct Crustal Protoliths of Roberts Victor Type I and II Eclogites. *Journal of Petrology* 62, egab090. https://doi.org/10.1093/petrology/egab090

Hasterok, D., Chapman, D.S. (2011) Heat production and geotherms for the continental lithosphere. *Earth and Planetary Science Letters* 307, 59–70. https://doi.org/10.1016/j.epsl.2011.04.034

Ickert, R.B., Stern, R.A. (2013) Matrix Corrections and Error Analysis in High-Precision SIMS $^{18}O/^{16}O$ Measurements of Ca-Mg-Fe Garnet. *Geostandards and Geoanalytical Research* 37, 429–448. https://doi.org/10.1111/j.1751-908X.2013.00222.x

Ickert, R.B., Stachel, T., Stern, R.A., Harris, J.W. (2015) Extreme ^{18}O-enrichment in majorite constrains a crustal origin of transition zone diamonds. *Geochemical Perspectives Letters* 1, 65–74. https://doi.org/10.7185/geochemlet.1507

Jacob, D.E. (2004) Nature and origin of eclogite xenoliths from kimberlites. *Lithos* 77, 295–316. https://doi.org/10.1016/j.lithos.2004.03.038

Kaminsky, F. (2012) Mineralogy of the lower mantle: A review of 'super-deep' mineral inclusions in diamond. *Earth-Science Reviews* 110, 127–147. https://doi.org/10.1016/j.earscirev.2011.10.005

Kaminsky, F., Zakharchenko, O., Davies, R., Griffin, W., Khachatryan-Blinova, G., Shiryaev, A. (2001) Superdeep diamonds from the Juina area, Mato Grosso State, Brazil. *Contributions to Mineralogy and Petrology* 140, 734–753. https://doi.org/10.1007/s004100000221

Kaminsky, F.V., Khachatryan, G.K., Andreazza, P., Araujo, D., Griffin, W.L. (2009) Super-deep diamonds from kimberlites in the Juina area, Mato Grosso State, Brazil. *Lithos* 112, 833–842. https://doi.org/10.1016/j.lithos.2009.03.036

Kaminsky, F., Matzel, J., Jacobsen, B., Hutcheon, I., Wirth, R. (2016) Isotopic fractionation of oxygen and carbon in decomposed lower-mantle inclusions in diamond. *Mineralogy and Petrology* 110, 379–385. https://doi.org/10.1007/s00710-015-0401-7

Kanzaki, M., Stebbins, J.F., Xue, X. (1991) Characterization of quenched high pressure phases in $CaSiO_3$ system by XRD and ^{29}Si NMR. *Geophysical Research Letters* 18, 463–466. https://doi.org/10.1029/91GL00463

Katsura, T., Yoneda, A., Yamazaki, D., Yoshino, T., Ito, E. (2010) Adiabatic temperature profile in the mantle. *Physics of the Earth and Planetary Interiors* 183, 212–218. https://doi.org/10.1016/j.pepi.2010.07.001

Knoche, R., Angel, R.J., Seifert, F., Fliervoet, T.F. (1998) Complete substitution of Si for Ti in titanite $Ca(Ti_{1-x}Si_x)^{VI}Si^{IV}O_5$. *American Mineralogist* 83, 1168–1175. http://minsocam.org/MSA/ammin/toc/Articles_Free/1998/Knoche_p1168-1175_98.pdf

Kopylova, M.G., Beausoleil, Y., Goncharov, A., Burgess, J., Strand, P. (2016) Spatial distribution of eclogite in the Slave cratonic mantle: The role of subduction. *Tectonophysics* 672–673, 87–103. https://doi.org/10.1016/j.tecto.2016.01.034

Korolev, N., Kopylova, M., Gurney, J.J., Moore, A.E., Davidson, J. (2018a) The origin of Type II diamonds as inferred from Cullinan mineral inclusions. *Mineralogy and Petrology* 112, 275–289. https://doi.org/10.1007/s00710-018-0601-z

Korolev, N.M., Kopylova, M., Bussweiler, Y., Pearson, D.G., Gurney, J., Davidson, J. (2018b) The uniquely high-temperature character of Cullinan diamonds: A signature of the Bushveld mantle plume? *Lithos* 304–307, 362–373. https://doi.org/10.1016/j.lithos.2018.02.011

Locock, A.J. (2008) An Excel spreadsheet to recast analyses of garnet into end-member components, and a synopsis of the crystal chemistry of natural silicate garnets. *Computers & Geosciences* 34, 1769–1780. https://doi.org/10.1016/j.cageo.2007.12.013

Mattey, D., Lowry, D., Macpherson, C. (1994) Oxygen isotope composition of mantle peridotite. *Earth and Planetary Science Letters* 128, 231–241. https://doi.org/10.1016/0012-821X(94)90147-3

Mikhailenko, D.S., Aulbach, S., Korsakov, A.V., Xu, Y.-G., Kaminsky, F.V. (2022) Titanite in Coesite-Kyanite-Bearing Eclogite from Kimberlite Pipe Udachnaya. *Doklady Earth Sciences* 503, 168–174. https://doi.org/10.1134/S1028334X22040122

Nakamura, D. (2009) A new formulation of garnet-clinopyroxene geothermometer based on accumulation and statistical analysis of a large experimental data set. *Journal of Metamorphic Geology* 27, 495–508. https://doi.org/10.1111/j.1525-1314.2009.00828.x

Nestola, F., Korolev, N., Kopylova, M., Rotiroti, N., Pearson, D.G., Pamato, M.G., Alvaro, M., Peruzzo, L., Gurney, J.J., Moore, A.E., Davidson, J. (2018) $CaSiO_3$ perovskite in diamond indicates the recycling of oceanic crust into the lower mantle. *Nature* 555, 237–241. https://doi.org/10.1038/nature25972

Pouchou, J.-L., Pichoir, F. (1991) Quantitative Analysis of Homogeneous or Stratified Microvolumes Applying the Model "PAP." In: Heinrich, K.F.J., Newbury, D.E. (Eds.) *Electron Probe Quantitation*. Springer, Boston, 31–75. https://doi.org/10.1007/978-1-4899-2617-3_4

Smith, E.M., Kopylova, M.G., Frezotti, M.L., Afanasiev, V.P. (2015) Fluid inclusions in Ebelyakh diamonds: Evidence of CO_2 liberation in eclogite and the effect of H_2O on diamond habit. *Lithos* 216–217, 106–117. https://doi.org/10.1016/j.lithos.2014.12.010

Sturm, R. (2002) PX-NOM—an interactive spreadsheet program for the computation of pyroxene analyses derived from the electron microprobe. *Computers & Geosciences* 28, 473–483. https://doi.org/10.1016/S0098-3004(01)00083-8

Timmerman, S., Spivak, A.V., Jones, A.P. (2021) Carbonatitic Melts and Their Role in Diamond Formation in the Deep Earth. *Elements* 17, 321–326. https://doi.org/10.2138/gselements.17.5.321

Vho, A., Lanari, P., Rubatto, D. (2019) An Internally-Consistent Database for Oxygen Isotope Fractionation Between Minerals. *Journal of Petrology* 60, 2101–2129. https://doi.org/10.1093/petrology/egaa001

Warr, L.N. (2021) IMA–CNMNC approved mineral symbols. *Mineralogical Magazine* 85, 291–320. https://doi.org/10.1180/mgm.2021.43

Yu, Y.G., Wentzcovitch, R.M., Vinograd, V.L., Angel, R.J. (2011) Thermodynamic properties of $MgSiO_3$ majorite and phase transitions near 660 km depth in $MgSiO_3$ and Mg_2SiO_4: A first principles study. *Journal of Geophysical Research: Solid Earth* 116, B02208. https://doi.org/10.1029/2010JB007912

Zedgenizov, D., Rubatto, D., Shatsky, V., Ragozin, A., Kalinina, V. (2016) Eclogitic diamonds from variable crustal protoliths in the northeastern Siberian craton: Trace elements and coupled $\delta^{13}C$–$\delta^{18}O$ signatures in diamonds and garnet inclusions. *Chemical Geology* 422, 46–59. https://doi.org/10.1016/j.chemgeo.2015.12.018

Zhang, J., Li, B., Utsumi, W., Liebermann, R.C. (1996) In situ X-ray observations of the coesite-stishovite transition: reversed phase boundary and kinetics. *Physics and Chemistry of Minerals* 23, 1–10. https://doi.org/10.1007/BF00202987